

# Provable Advantage of Parameterized Quantum Circuit in Function Approximation

Zhan Yu,<sup>1,2</sup> Qiu hao Chen,<sup>1</sup> Yuling Jiao,<sup>1,3</sup> Yinan Li,<sup>1,3,\*</sup>  
Xiliang Lu,<sup>1,3</sup> Xin Wang,<sup>4</sup> and Jerry Zhijian Yang<sup>1,3</sup>

<sup>1</sup>*School of Mathematics and Statistics, Wuhan University, Wuhan 430072, China*

<sup>2</sup>*Centre for Quantum Technologies, National University of Singapore, 117543, Singapore*

<sup>3</sup>*Hubei Key Laboratory of Computational Science, Wuhan 430072, China*

<sup>4</sup>*Thrust of Artificial Intelligence, Information Hub,*

*Hong Kong University of Science and Technology (Guangzhou), Guangzhou 511453, China*

(Dated: October 12, 2023)

Understanding the power of parameterized quantum circuits (PQCs) in accomplishing machine learning tasks is one of the most important questions in quantum machine learning. In this paper, we analyze the expressivity of PQCs through the lens of function approximation. Previously established universal approximation theorems for PQCs are mainly nonconstructive, leading us to the following question: How large do the PQCs need to be to approximate the target function up to a given error? We exhibit explicit constructions of data re-uploading PQCs for approximating continuous and smooth functions and establish quantitative approximation error bounds in terms of the width, the depth and the number of trainable parameters of the PQCs. To achieve this, we utilize techniques from quantum signal processing and linear combinations of unitaries to construct PQCs that implement multivariate polynomials. We implement global and local approximation techniques using Bernstein polynomials and local Taylor expansion and analyze their performances in the quantum setting. We also compare our proposed PQCs to nearly optimal deep neural networks in approximating high-dimensional smooth functions, showing that the ratio between model sizes of PQC and deep neural networks is exponentially small with respect to the input dimension. This suggests a potentially novel avenue for showcasing quantum advantages in quantum machine learning.

## I. INTRODUCTION

In quantum computing, one key area of interest is to investigate if quantum computers could accelerate classical machine learning tasks in data analysis and artificial intelligence, giving rise to an interdisciplinary field known as *quantum machine learning* [1]. As the quantum analogs of classical neural networks, *parameterized quantum circuits* (PQCs) [2] have gained significant attention as a prominent paradigm to yield quantum advantages. PQCs offer a concrete and practical way to implement quantum machine learning algorithms in noisy and intermediate-scale quantum (NISQ) devices [3], rendering them well-suited for a diverse array of tasks [4–11].

To establish the practical significance of quantum machine learning, an ongoing pursuit is to demonstrate their superiority in solving real-world learning problems compared to classical learning models, including the most commonly used deep neural networks [12]. For typical supervised learning tasks, such as image classification and price prediction, the goal is to construct a model to learn a mapping function from the input to output via training data sets. Their essential mathematical forms are approximating high-dimensional functions. Powerful tools from approximation theory provide fruitful mathematical frameworks for understanding the “black magic” of deep learning by establishing approximation error bounds of deep neural networks in terms of *width*, *depth*, and *the number of weights and neurons*, see e.g. Refs. [13–19] and references therein.

Substantial investigations have showcased the power of quantum machine learning for specific learning tasks [20–27]. In particular, recently proposed data re-uploading models [11, 28] have been shown to have universal approximation properties [29–32] and strong learning performances [26], making it a suitable

\* [Yinan.Li@whu.edu.cn](mailto:Yinan.Li@whu.edu.cn)

quantum machine model for supervised learning tasks. However, it remains an open question whether some quantum advantages could be gained from data re-uploading PQCs. Is it possible to demonstrate the power of PQC models from the perspective of function approximation? For instance, would it be possible to utilize quantum models to approximate functions that are inefficient to approximate through classical neural networks? To bring quantum machine learning models forward via this route, the main challenge lies in determining the necessary size of PQCs to achieve a desired level of approximation error. This could be a new venue for proving rigorous quantum advantages for quantum machine learning algorithms.

In this paper, we analyze the approximation abilities of data re-uploading PQCs for a wide range of functions and characterize the approximation error in terms of the number of qubits (width), the depth of the circuits and the number of trainable parameters/gates, in analogy to the classical setting. Our main contributions are *explicit PQCs for point-wisely approximating smooth functions and quantitative bounds for their approximation error*. We start with explicitly constructing multi-qubit data re-uploading PQCs to implement multivariate polynomials. Following this, we prove the universality of PQCs on approximating Lipschitz continuous functions in a constructive way and prove quantitative approximation error bounds based on established results on Bernstein polynomials. For a more general class of Hölder smooth functions, we utilize the local Taylor expansion to achieve a piecewise approximation, following the techniques used in deep neural network approximations [16–19]. The key technique is to construct a PQC to localize the entire region into hypercubes of small size, then nest it with another PQC to implement the Taylor series. Finally, we arrive at the first quantitative error bounds for approximating general Hölder smooth functions via such nested PQCs. A glance at these PQC constructions is illustrated in Fig. 1.

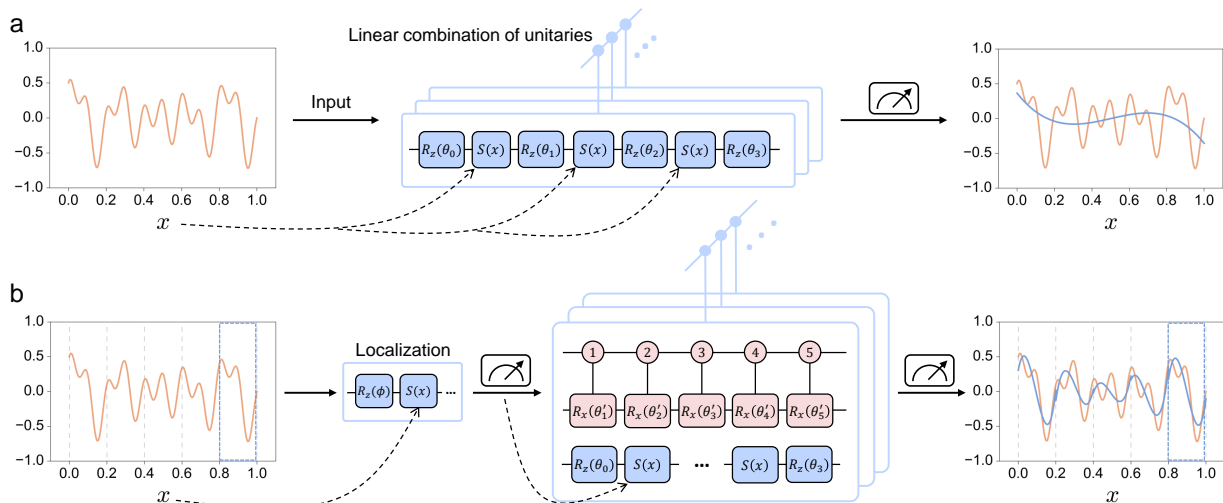


**FIG. 1. Overview of PQCs for approximating continuous functions.** (a) Flowchart illustrating the strategy for using PQCs to approximate continuous functions via implementing Bernstein polynomials. The input data  $x$  is encoded into the PQC through  $S(x)$ , with the PQC (blue background) capable of representing parity-constrained polynomials up to degree 3 (as  $x$  is encoded three times). The technique of linear combination of unitaries (LCU) is used to aggregate these polynomials together. The output of PQC derives from measurement with a specific observable. Fine-tuning trainable parameters in  $R_Z$  gates yields a polynomial output depicted in the right panel. (b) Flowchart illustrating the strategy of approximation via local Taylor expansions. We first apply a PQC to localize the input domain into  $K = 5$  regions. For example, for input  $x \in [0.8, 1]$ , PQC outputs  $x' = 0.8$  as a fixed point. Then  $x - x'$  will be fed into a new PQC for implementing the local Taylor expansions at the fixed point  $x'$ , forming a nesting architecture. Control gates with pink backgrounds implement the Taylor coefficients. Fine-tuning trainable parameters in  $R_X$  and  $R_Z$  gates yields a piecewise polynomial with degree 3 that approximates the target function.

All of our proposed PQCs are constructed explicitly without any assumption: They only use elementary gates such as CNOT and single-qubit rotations. We also compare our results on smooth function approxi-

mation to the nearly optimal results of classical deep neural network approximations. Notably, we find that in scenarios characterized by high-dimensional input data and target functions adhering to specific smoothness criteria, our PQCs demonstrate a rigorous quantum advantage over nearly optimal deep ReLU neural networks, quantified by both model size and number of trainable parameters. Specifically, the ratio between model sizes (the number of parameters) of PQC and deep ReLU neural networks is exponentially small with respect to the input dimension. Thus, our results can be seen as a first step towards exhibiting new quantum advantages for practical machine learning tasks from a mathematical perspective.

## II. RESULTS

### A. Framework setup

*a. Data re-uploading PQCs.* We start by reviewing data re-uploading PQCs and use a simple example to explain how they could approximate functions in a classical way. The data re-uploading PQC is a quantum circuit that consists of interleaved data encoding circuit blocks and trainable circuit blocks [11, 28]. More precisely, let  $\mathbf{x}$  be the input data vector and  $\boldsymbol{\theta} = (\boldsymbol{\theta}_0, \dots, \boldsymbol{\theta}_L)$  be a set of trainable parameter vectors.  $S(\mathbf{x})$  is a quantum circuit that encode  $\mathbf{x}$  and  $V(\boldsymbol{\theta}_j)$  is a trainable quantum circuit with trainable parameter vector  $\boldsymbol{\theta}_j$ . An  $L$ -layer data re-uploading PQC can be then expressed as

$$U_{\boldsymbol{\theta}}(\mathbf{x}) = V(\boldsymbol{\theta}_0) \prod_{j=1}^L S(\mathbf{x}) V(\boldsymbol{\theta}_j), \quad (1)$$

Applying  $U_{\boldsymbol{\theta}}(\mathbf{x})$  to an initial quantum state and measuring the output states provides a way to express functions on  $\mathbf{x}$ :

$$f_{U_{\boldsymbol{\theta}}}(\mathbf{x}) := \langle 0 | U_{\boldsymbol{\theta}}^{\dagger}(\mathbf{x}) \mathcal{O} U_{\boldsymbol{\theta}}(\mathbf{x}) | 0 \rangle, \quad (2)$$

where  $\mathcal{O}$  is some Hermitian observable. The *approximation capability* of the PQC  $U_{\boldsymbol{\theta}}(\mathbf{x})$  can be characterized by the classes of functions that  $f_{U_{\boldsymbol{\theta}}}(\mathbf{x})$  can approximate by tuning the trainable parameter vector  $\boldsymbol{\theta}$ . We then turn to an example of single-qubit PQCs approximating univariate functions. For the input  $x \in [-1, 1]$ , we utilized the Pauli  $X$  basis encoding scheme [10] and defined the data encoding operator as a Pauli  $X$  rotation  $S(x) := e^{i \arccos(x) X}$ . Interleaving the data encoding unitary  $S(x)$  with some parameterized Pauli  $Z$  rotations  $R_Z(\theta)$  gives the circuit of data re-uploading PQC for one variable as  $U_{\boldsymbol{\theta}}(x) := R_Z(\theta_0) \prod_{j=1}^L S(x) R_Z(\theta_j)$  where  $\boldsymbol{\theta} = (\theta_0, \dots, \theta_L) \in \mathbb{R}^{L+1}$  is a set of trainable parameters. Utilizing results from quantum signal processing [33–35], there exists  $\boldsymbol{\theta} \in \mathbb{R}^{L+1}$  such that  $U_{\boldsymbol{\theta}}(x)$  implements polynomial transformations  $p(x) \in \mathbb{R}[x]$  as  $p(x) = \langle + | U_{\boldsymbol{\theta}}(x) | + \rangle$  for any  $x \in [-1, 1]$  if and only if the degree of  $p(x)$  is at most  $L$ , the parity of  $p(x)$  is  $L \bmod 2$ <sup>1</sup>, and  $|p(x)| \leq 1$  for all  $x \in [-1, 1]$ . Then univariate functions that could be approximated by the specified polynomial  $p(x)$  could also be approximated by the PQC  $U_{\boldsymbol{\theta}}(x)$ . Other than the real polynomials, there are also types of single-qubit PQC with Pauli  $Z$  basis encoding that could implement complex trigonometric polynomials [31].

*b. Explicit construction of PQCs for multivariate polynomials.* Although PQCs for approximate univariate functions have been constructed and analyzed, it has not yet been generally extended to the case of multivariate functions. Current proofs of universal approximation for multivariate functions are nonconstructive [29, 32] and require arbitrary circuit width, arbitrary multi-qubit global parameterized unitaries, and arbitrary observables. Goto *et al.* [36] proposed several constructions for approximating multivariate functions with the assistance of parameterized data pre-processing and post-processing, yielding a quantum-enhanced hybrid scheme rather than a purely quantum setting.

<sup>1</sup> A polynomial  $p(x)$  has parity 0 if all coefficients corresponding to odd powers of  $x$  are 0, and similarly  $p(x)$  has parity 1 if all coefficients corresponding to even powers of  $x$  are 0.

We now move to our explicit construction of PQCs for multivariate polynomials. A multivariate polynomial with  $d$  variables and degree  $s$  is defined as  $p(\mathbf{x}) := \sum_{\|\alpha\|_1 \leq s} c_\alpha \mathbf{x}^\alpha$  where  $\mathbf{x}^\alpha = x_1^{\alpha_1} x_2^{\alpha_2} \cdots x_d^{\alpha_d}$ . To implement the multivariate polynomial  $p(\mathbf{x})$ , we first build a PQC to express a monomial  $c_\alpha \mathbf{x}^\alpha$ . The construction is a trivial extension of the univariate case: We simply apply the single-qubit PQC with Pauli  $X$  basis encoding on each  $x_j$  to implement  $x_j^{\alpha_j}$  for  $1 \leq j \leq d$ , respectively. The coefficient  $c_\alpha \in \mathbb{R}$  could be implemented by any of these PQCs. Thus we could construct a PQC  $U^\alpha(\mathbf{x}) := \bigotimes_{j=1}^d U_{\theta_j}(x_j)$  such that  $\langle + |^{\otimes d} U^\alpha(\mathbf{x}) | + \rangle^{\otimes d} = c_\alpha \mathbf{x}^\alpha$ . The depth of the PQC  $U^\alpha(\mathbf{x})$  is at most  $2s + 1$ , the width is at most  $d$ , and the number of parameters is at most  $s + d$ .

Having PQCs that implement monomials, the next step is to aggregate monomials to implement the multivariate polynomial. A natural idea is to sum the monomial PQCs together as  $U_p(\mathbf{x}) = \sum_{\|\alpha\|_1 \leq s} U^\alpha(\mathbf{x})$ . However, the addition operation in quantum computing is non-trivial as the sum of unitary operators is not necessarily unitary. To overcome this issue, we utilize *linear combination of unitaries* (LCU) [37] to implement the operator  $U_p(\mathbf{x})$  on a quantum computer. Realizing the linear combination of PQCs  $U^\alpha(\mathbf{x})$  requires applying multi-qubit control on each  $U^\alpha(\mathbf{x})$ , which could be further decomposed into linear-depth quantum circuits of CNOT gates and single-qubit rotation gates without using any ancilla qubit [38]. Then we can obtain the polynomial  $p(\mathbf{x}) = \langle + |^{\otimes d} U_p(\mathbf{x}) | + \rangle^{\otimes d}$  by applying the Hadamard test on the LCU circuit. Summarizing the above, we establish the following proposition about using PQCs for implementing multivariate polynomials. A formal description of such PQCs is given in Appendix B.

**Proposition 1.** *For any multivariate polynomial  $p(\mathbf{x})$  with  $d$  variables and degree  $s$  such that  $|p(\mathbf{x})| \leq 1$  for  $\mathbf{x} \in [0, 1]^d$ , there exists a PQC  $W_p(\mathbf{x})$  such that*

$$f_{W_p}(\mathbf{x}) := \langle 0 | W_p^\dagger(\mathbf{x}) Z^{(0)} W_p(\mathbf{x}) | 0 \rangle = p(\mathbf{x}) \quad (3)$$

where  $Z^{(0)}$  is the Pauli  $Z$  observable on the first qubit. The width of the PQC is  $O(d + \log s + s \log d)$ , the depth is  $O(s^2 d^s (\log s + s \log d))$ , and the number of parameters is  $O(sd^s(s + d))$ .

Note that the initial state in the Hadamard test is  $|0\rangle^{\otimes d}$  since  $|+\rangle^{\otimes d}$  could be easily prepared by applying Hadamard gates on  $|0\rangle^{\otimes d}$ . Measuring the first qubit of  $W_p(\mathbf{x})$  for  $O(\frac{1}{\varepsilon^2})$  times is needed to estimate the value of  $p(\mathbf{x})$  up to an additive error  $\varepsilon$ . We could further use the amplitude estimation algorithm [39] to reduce the overhead while increasing the circuit depth by  $O(\frac{1}{\varepsilon})$ .

## B. PQC approximation for continuous functions

Polynomials play a central role in approximation theory. The celebrated Weierstrass approximation theorem (see e.g. [40, Sec. 10.2.2]) indicates that polynomials are sufficient to approximate continuous univariate functions. For multivariate functions, their approximation can be implemented using Bernstein polynomials [41, 42]. We shall utilize these results to prove approximation error bounds for using PQCs to approximate multivariate Lipschitz continuous functions.

For a  $d$ -variable continuous function  $f : [0, 1]^d \rightarrow \mathbb{R}$ , the multivariate Bernstein polynomial with degree  $n \in \mathbb{N}^+$  of  $f$  is defined as

$$B_n(\mathbf{x}) := \sum_{k_1=0}^n \cdots \sum_{k_d=0}^n f\left(\frac{\mathbf{k}}{n}\right) \prod_{j=1}^d \binom{n}{k_j} x_j^{k_j} (1 - x_j)^{n-k_j}, \quad (4)$$

where  $\mathbf{k} = (k_1, \dots, k_d) \in \{0, \dots, n\}^d$ . It is known that Bernstein polynomials converge uniformly to  $f$  on  $[0, 1]^d$  as  $n \rightarrow \infty$  [41, 42]. The PQC constructed in Proposition 1 could implement the Bernstein polynomial with proper rescaling, which implies that the PQC is a universal approximator for any bounded continuous functions.

**Theorem 1** (The Universal Approximation Theorem of PQC). *For any continuous function  $f : [0, 1]^d \rightarrow [-1, 1]$ , given an  $\varepsilon > 0$ , there exist an  $n \in \mathbb{N}$  and a PQC  $W_b(\mathbf{x})$  with width  $O(d \log n)$ , depth  $O(dn^d \log n)$  and the number of trainable parameters  $O(dn^d)$  such that*

$$|f(\mathbf{x}) - f_{W_b}(\mathbf{x})| \leq \varepsilon \quad (5)$$

for all  $\mathbf{x} \in [0, 1]^d$ , where  $f_{W_b}(\mathbf{x}) := \langle 0 | W_b^\dagger(\mathbf{x}) Z^{(0)} W_b(\mathbf{x}) | 0 \rangle$ .

The PQCs that universally approximate continuous functions are explicitly constructed without any impractical assumption, improving the previous results presented in Refs. [29, 32]. Moreover, for continuous functions  $f$  satisfying the Lipschitz condition,  $|f(\mathbf{x}) - f(\mathbf{y})| \leq \ell \|\mathbf{x} - \mathbf{y}\|_\infty$  for any  $\mathbf{x}, \mathbf{y}$ , the approximation rate of Bernstein polynomials could be quantitatively characterized in terms of the degree  $n$ , the number of variables  $d$  and the Lipschitz constant  $\ell$  [42]. Thus a quantitative error bound for PQC approximating Lipschitz continuous functions could be obtained as follows.

**Theorem 2.** *Given a Lipschitz continuous function  $f : [0, 1]^d \rightarrow [-1, 1]$  with a Lipschitz constant  $\ell$ , for any  $\varepsilon > 0$  and  $n \in \mathbb{N}$ , there exists a PQC  $W_b(\mathbf{x})$  with such that  $f_{W_b}(\mathbf{x}) := \langle 0 | W_b^\dagger(\mathbf{x}) Z^{(0)} W_b(\mathbf{x}) | 0 \rangle$  satisfies*

$$|f(\mathbf{x}) - f_{W_b}(\mathbf{x})| \leq \varepsilon + 2 \left( \left( 1 + \frac{\ell^2}{n\varepsilon^2} \right)^d - 1 \right) \leq \varepsilon + d2^d \frac{\ell^2}{n\varepsilon^2} \quad (6)$$

for all  $\mathbf{x} \in [0, 1]^d$ . The width of the PQC is  $O(d \log n)$ , the depth is  $O(dn^d \log n)$ , and the number of parameters is  $O(dn^d)$ .

We prove these theorems in Appendix C. Although a quantitative approximation error bound is characterized in Theorem 2, we could find that  $n$  has to be sufficiently large in order to obtain a good precision, yielding an extremely deep PQC. This inefficiency is essentially due to the intrinsic difficulty of using a single global polynomial to uniformly approximate a continuous function. A possible approach that may overcome the obstacle is to use local polynomials to achieve a piecewise approximation, which we will discover in the next section.

### C. PQC approximation for Hölder smooth functions

To achieve a piecewise approximation of multivariate functions, we follow the path of classical deep neural networks approximation [16, 18, 43], which utilizes multivariate Taylor series to approximate target functions in small local regions.

We focus on Hölder smooth functions. Let  $\beta = s + r > 0$ , where  $r \in (0, 1]$  and  $s \in \mathbb{N}^+$ . For a finite constant  $B_0 > 0$ , the  $\beta$ -Hölder class of functions  $\mathcal{H}^\beta([0, 1]^d, B_0)$  is defined as

$$\mathcal{H}^\beta([0, 1]^d, B_0) = \left\{ f : [0, 1]^d \rightarrow \mathbb{R}, \max_{\|\alpha\|_1 \leq s} \|\partial^\alpha f\|_\infty \leq B_0, \max_{\|\alpha\|_1 = s} \sup_{\mathbf{x} \neq \mathbf{y}} \frac{|\partial^\alpha f(\mathbf{x}) - \partial^\alpha f(\mathbf{y})|}{\|\mathbf{x} - \mathbf{y}\|_2^r} \leq B_0 \right\}, \quad (7)$$

where  $\partial^\alpha = \partial^{\alpha_1} \dots \partial^{\alpha_d}$  for  $\alpha = (\alpha_1, \dots, \alpha_d) \in \mathbb{N}^d$ . We note that Hölder smooth functions are natural generalizations of various continuous functions: When  $\beta \in (0, 1)$ ,  $f$  is Hölder continuous with order  $\beta$  and Hölder constant  $B_0$ ; when  $\beta = 1$ ,  $f$  is Lipschitz continuous with Lipschitz constant  $B_0$ ; when  $1 < \beta \in \mathbb{N}$ ,  $f \in C^s([0, 1]^d)$ , the class of  $s$ -smooth functions whose  $s$ -th partial derivatives exist and are bounded. As shown in Petersen and Voigtlaender [16], for any  $\beta$ -Hölder smooth function  $f \in \mathcal{H}^\beta([0, 1]^d, B_0)$ , its local Taylor expansion at some fixed point  $\mathbf{x}_0 \in [0, 1]^d$  satisfies

$$\left| f(\mathbf{x}) - \sum_{\|\alpha\|_1 \leq s} \frac{\partial^\alpha f(\mathbf{x}_0)}{\alpha!} (\mathbf{x} - \mathbf{x}_0)^\alpha \right| \leq d^s \|\mathbf{x} - \mathbf{x}_0\|_2^\beta \quad (8)$$

for all  $\mathbf{x} \in [0, 1]^d$ , where  $\alpha! = \alpha_1! \dots \alpha_d!$ . Next, we show how to construct PQCs to implement the Taylor expansion of  $\beta$ -Hölder functions in the following three steps.

*a. Localization.* To utilize the Hölder smoothness, we need to first localize the entire region  $[0, 1]^d$ . Given  $K \in \mathbb{N}$  and  $\Delta \in (0, \frac{1}{3K})$ , for each  $\boldsymbol{\eta} = (\eta_1, \dots, \eta_d) \in \{0, 1, \dots, K-1\}^d$ , we define

$$Q_{\boldsymbol{\eta}} := \left\{ \mathbf{x} = (x_1, \dots, x_d) : x_i \in \left[ \frac{\eta_i}{K}, \frac{\eta_i + 1}{K} - \Delta \cdot \mathbf{1}_{\eta_i < K-1} \right] \right\}. \quad (9)$$

By the definition of  $Q_{\boldsymbol{\eta}}$ , the region  $[0, 1]^d$  is approximately divided into small hypercubes  $\bigcup_{\boldsymbol{\eta}} Q_{\boldsymbol{\eta}}$  and some trifling region  $\Lambda(d, K, \Delta) := [0, 1]^d \setminus (\bigcup_{\boldsymbol{\eta}} Q_{\boldsymbol{\eta}})$ , as illustrated in Fig. 2.

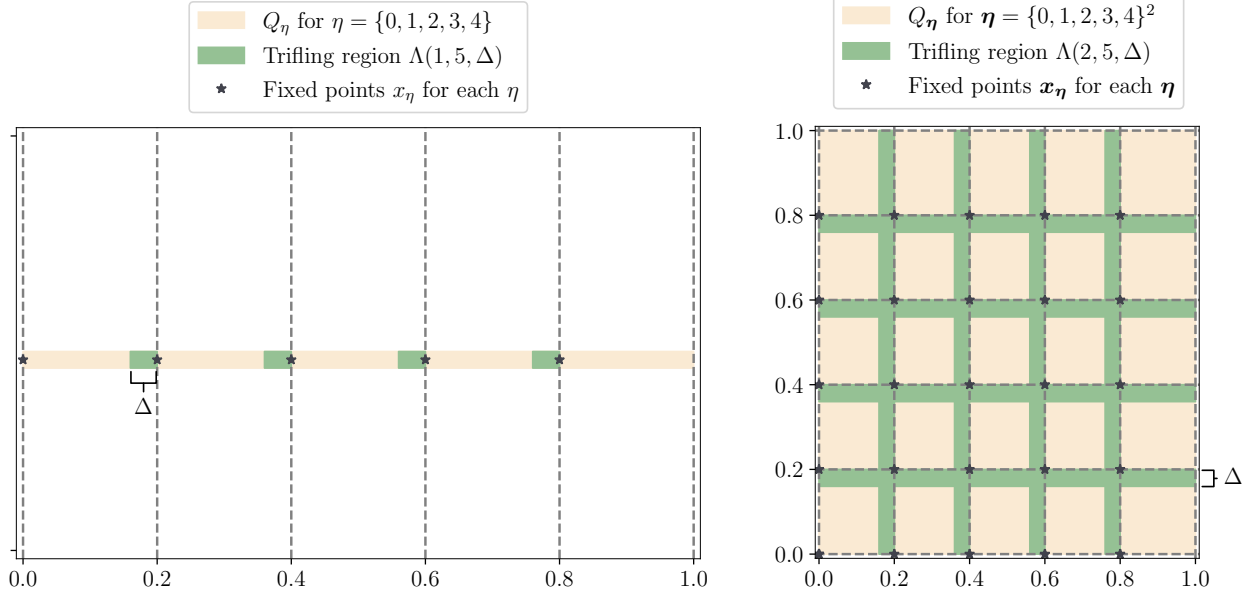


FIG. 2. **An illustration of localization.** The left panel demonstrates the localization  $\bigcup_{\boldsymbol{\eta}} Q_{\boldsymbol{\eta}}$  for  $K = 5$  and  $d = 1$ . The right panel shows the case of localization for  $K = 5$  and  $d = 2$ . The “volume” of the trifling region  $\Lambda(d, K, \Delta)$  is no more than  $dK\Delta$ .

We construct a PQC that maps all  $\mathbf{x} \in Q_{\boldsymbol{\eta}}$  to some fixed point  $\mathbf{x}_{\boldsymbol{\eta}} = \frac{\boldsymbol{\eta}}{K}$  in  $Q_{\boldsymbol{\eta}}$ , i.e., approximating the piecewise-constant function  $D(\mathbf{x}) = \frac{\boldsymbol{\eta}}{K}$  if  $\mathbf{x} \in Q_{\boldsymbol{\eta}}$ . We describe our construction for  $d = 1$ , where  $D(x) = \frac{k}{K}$  if  $x \in [\frac{k}{K}, \frac{k+1}{K} - \Delta \cdot \mathbf{1}_{k < K-1}]$  for  $k = 0, \dots, K-1$ . The multivariate case could be naturally generalized by applying  $D(x)$  to each variable  $x_j$ . The idea is to construct a polynomial that approximates the function  $D(x)$  based on the polynomial approximation to the sign function [44], which can then be implemented by a single-qubit PQC. Generalizing to the multivariate localization, there exists a PQC  $W_D(\mathbf{x})$  of depth  $O(\frac{1}{\Delta} \log \frac{K}{\varepsilon})$  and width  $O(d)$  such that the output  $f_{W_D}(\mathbf{x})$  maps  $\mathbf{x}$  to the corresponding fixed point  $\mathbf{x}_{\boldsymbol{\eta}}$  with precision  $\varepsilon$ . We can obtain an estimation of  $\boldsymbol{\eta}$  using  $\lfloor K f_{W_D}(\mathbf{x}) \rfloor$ .

*b. Implementing the Taylor coefficients.* Next, we use PQC to implement the Taylor coefficients  $\xi_{\boldsymbol{\eta}, \alpha} := \frac{\partial^\alpha f(\mathbf{x}_{\boldsymbol{\eta}})}{\alpha!} \in [-1, 1]$  for each  $\boldsymbol{\eta} = (\eta_1, \dots, \eta_d) \in \{0, 1, \dots, K-1\}^d$  and  $\alpha$ , which is essentially a point-fitting problem. Then we could construct a PQC  $U_{co}^\alpha = \sum_{\boldsymbol{\eta}} |\boldsymbol{\eta}\rangle \langle \boldsymbol{\eta}| \otimes R_X(\theta_{\boldsymbol{\eta}, \alpha})$  such that  $\langle \boldsymbol{\eta}, 0 | U_{co}^\alpha | \boldsymbol{\eta}, 0 \rangle = \xi_{\boldsymbol{\eta}, \alpha}$ , where  $|\boldsymbol{\eta}\rangle = |\eta_1\rangle \otimes \dots \otimes |\eta_d\rangle$  and  $\theta_{\boldsymbol{\eta}, \alpha} = 2 \arccos(\xi_{\boldsymbol{\eta}, \alpha})$ . The depth of  $U_{co}^\alpha$  is  $O(K^d)$ , the width is  $O(d \log K)$ , and the number of parameters is  $O(K^d)$ . Note that the state  $|\boldsymbol{\eta}\rangle$  can be prepared using basis encoding on the provided  $\boldsymbol{\eta} = \lfloor K f_{W_D}(\mathbf{x}) \rfloor$  from the localization step.

*c. Implementing multivariate Taylor series.* To implement the multivariate Taylor expansion of a function at some fixed point  $\mathbf{x}_{\boldsymbol{\eta}}$ , we first build a PQC to represent a single term in the Taylor series, which could be done by combining the PQC which implements the Taylor coefficients and the PQC which implements monomials, i.e., constructing  $U_{\boldsymbol{\eta}}^\alpha(\mathbf{x}) := U_{co}^\alpha \otimes U^\alpha(\mathbf{x} - \mathbf{x}_{\boldsymbol{\eta}})$ . The depth of  $U_{\boldsymbol{\eta}}^\alpha(\mathbf{x})$  is  $O(K^d + s)$ , the

width is  $O(d \log K)$ , and the number of parameters is at most  $K^d + s + d$ . The next step is to aggregate single Taylor terms together to implement the truncated Taylor expansion of the target function. We use LCU to construct the PQC  $U_t(\mathbf{x}, \mathbf{x}_\eta) := \sum_{\|\alpha\|_1 \leq s} U_\eta^\alpha(\mathbf{x})$ , so that we can implement the Taylor expansion of the function  $f$  at point  $\mathbf{x}_\eta$  as  $\langle \boldsymbol{\eta}, 0 | \langle + |^{\otimes d} U_t(\mathbf{x}, \mathbf{x}_\eta) | \boldsymbol{\eta}, 0 \rangle | + \rangle^{\otimes d}$ .

We construct a nested PQC as  $U_t(\mathbf{x}, f_{W_D}(\mathbf{x}))$ , such that for any input  $\mathbf{x}$ , the corresponding fixed point could be determined by the localization PQC. Such a PQC could be used, together with the Hadamard test, to approximate Hölder smooth functions. In particular, we prove the approximation error bound of our constructed PQC based on the error rate of Taylor expansion in Eq. (8).

**Theorem 3.** *Given a function  $f \in \mathcal{H}^\beta([0, 1]^d, 1)$  with  $\beta = r + s$ ,  $r \in (0, 1]$  and  $s \in \mathbb{N}^+$ , for any  $K \in \mathbb{N}$  and  $\Delta \in (0, \frac{1}{3K})$ , there exists a PQC  $W_t(\mathbf{x})$  such that  $f_{W_t}(\mathbf{x}) := \langle 0 | W_t^\dagger(\mathbf{x}) Z^{(0)} W_t(\mathbf{x}) | 0 \rangle$  satisfies*

$$|f(\mathbf{x}) - f_{W_t}(\mathbf{x})| \leq d^{s+\beta/2} K^{-\beta} \quad (10)$$

for  $\mathbf{x} \in \bigcup_\eta Q_\eta$ . The width of the PQC is  $O(d \log K + \log s + s \log d)$ , the depth is  $O(s^2 d^s K^d (\log s + s \log d + d \log K)) + \frac{1}{\Delta} \log K$ , and the number of parameters is  $O(sd^s(s + d + K^d))$ .

The proof can be found in Appendix D. Note that the PQC in Theorem 3 consists of two nested parts and its depth is counted as the sum of two PQCs for simplicity. We have established the uniform convergence property of PQCs for approximating Hölder smooth function on  $[0, 1]^d$  except for the trifling region  $\Lambda(d, K, \Delta)$ . The Lebesgue measure of such a trifling region is no more than  $dK\Delta$ . We can set  $\Delta = K^{-d}$  with no influence on the size of the constructed PQC, and a similar approximation error bound in the entire region  $[0, 1]^d$  under the  $L^2$  distance could be obtained.

### III. DISCUSSION

To the best of our knowledge, our results establish the first explicit PQC constructions for approximating Lipschitz continuous and Hölder smooth functions with quantitative approximation error bounds. These results open up the possibility of comparing the size of PQCs and the size of classical deep neural networks for accomplishing the same function approximation tasks and see if there is any quantum advantage in terms of the model size and the number of trainable parameters. Here we mainly focus on the comparison with the results of approximation errors of classical machine learning models. In classical deep learning, the deep feed-forward neural network (FNN) equipped with the rectified linear unit (ReLU) activation function is one of the most commonly used models. The quantitative approximation error bounds of ReLU FNNs for approximating continuous functions have been recently established, including the nearly optimal approximation error bounds of ReLU FNNs for smooth functions [18]. Here we briefly compare the approximation errors of PQCs and ReLU FNNs in terms of width, depth and the number of trainable parameters. Detailed comparisons can be found in Appendix E.

For simplicity, we consider smooth functions in  $C^s([0, 1]^d)$  with smooth index  $s \in \mathbb{N}$  as the target functions in our comparison. Smooth functions with smooth index  $s$  are exactly  $s$ -Hölder continuous functions. Here we consider the scenario that the smooth index  $s$  of the target function is small and the dimension of the input data  $d$  is substantially large (i.e.  $d \gg s$ ), which holds relevance in numerous real-world applications (e.g., the input dimension  $d$  is 784 for the MNIST dataset and is 150, 528 for the ImageNet dataset [45], and empirically  $s \leq 10$ ). In this case, a ReLU FNN with width  $O(s^d K^{\lambda_0 d/2})$ , depth  $O(K^{(1-\lambda_0)d/2})$ , and the number of trainable parameters  $O(s^d K^{(1+\lambda_0)d/2})$  can achieve an approximation error in  $O(s^d K^{-s})$ , where  $\lambda_0$  quantifies the width of the FNN and  $K$  denotes the number of partitions within the interval  $[0, 1]$  for localization. In the quantum setting, the PQC proposed in Theorem 3 with width  $O(d \log K)$ , depth  $O(d^s K^d)$  and the number of trainable parameters  $O(d^s K^d)$  could achieve an approximation error  $O(d^{3s/2} K^{-s})$ . We shall compare the model size (width  $\times$  depth) and the number of parameters between ReLU FNNs and PQCs

to achieve the same approximation error  $\varepsilon$ . Remarkably, we find that when the smoothness index of the target function is not too small, PQCs offer a distinct advantage over the nearly optimal ReLU FNN, i.e.,

$$\frac{\# \text{Parameters in PQC}}{\# \text{Parameters in FNN}}, \frac{\text{Width of PQC} \times \text{Depth of PQC}}{\text{Width of FNN} \times \text{Depth of FNN}} = O\left(\frac{1}{2^d}\right), \text{ when } s = \Omega(d^{3s/d}(1/\varepsilon)^{1/d}).$$

Note that the condition  $s = \Omega(d^{3s/d}(1/\varepsilon)^{1/d})$  is easily satisfied for large  $d$  and small  $s$ , since  $d^{3s/d} \approx 1$ . Thus, we believe such quantum advantages potentially exist in many practical scenarios.

Aiming to understand and continuously expand the range of problems that can be addressed using quantum machine learning, we have demonstrated the approximation capabilities of PQC models in supervised learning. We characterized the approximation error of PQCs in terms of the model size, delivering a deeper understanding of the expressive power of PQCs that is beyond the universal approximation properties. With these results, we can unlock the full potential of these models and drive advancements in quantum machine learning. Notably, by comparing our results with the near-optimal approximation error bound of classical ReLU neural networks, we demonstrate a rigorous quantum advantage over the classical models on approximating high-dimensional functions that satisfy specific smoothness criteria, quantified by an improvement on the model size and the number of parameters.

Unlike many other investigations in the universal approximation properties of PQC models [29, 30, 32, 36, 46], our constructions of PQCs for approximating broad classes of continuous functions do not rely on any impractical assumptions. All the variables take the form of parameters within single-qubit rotation gates, avoiding any classical parameterized pre-processing or post-processing. Ultimately, our research provides valuable insights into the theoretical underpinnings of PQCs in quantum machine learning and paves the way for leveraging its capabilities in machine learning for both classical and quantum applications.

In this work, we introduce a novel nested PQC structure, which significantly improves the approximation capabilities. Future work could focus on exploring more powerful PQC constructions based on our proposed idea and understanding the capabilities and limitations of PQCs in more practical tasks even with real-world data. It will also be interesting to develop efficient training strategies for PQCs, such as accelerated methods that achieve faster convergence rates.

## ACKNOWLEDGMENT

Part of this work was done when Z.Y. was visiting Wuhan University. This work is supported by the National Key Research and Development Program of China (No. 2020YFA0714200), the National Nature Science Foundation of China (No. 62302346, No. 12125103, No. 12071362, No. 12371424, No. 12371441) and supported by the ‘‘Fundamental Research Funds for the Central Universities’’.

- 
- [1] J. Biamonte, P. Wittek, N. Pancotti, P. Rebentrost, N. Wiebe, and S. Lloyd, Quantum machine learning, *Nature* **549**, 195 (2017).
  - [2] M. Benedetti, E. Lloyd, S. Sack, and M. Fiorentini, Parameterized quantum circuits as machine learning models, *Quantum Science and Technology* **4**, 043001 (2019).
  - [3] J. Preskill, Quantum Computing in the NISQ era and beyond, *Quantum* **2**, 79 (2018).
  - [4] A. Kandala, A. Mezzacapo, K. Temme, M. Takita, M. Brink, J. M. Chow, and J. M. Gambetta, Hardware-efficient variational quantum eigensolver for small molecules and quantum magnets, *Nature* **549**, 242 (2017).
  - [5] M. Cerezo, K. Sharma, A. Arrasmith, and P. J. Coles, Variational quantum state eigensolver, *npj Quantum Information* **8**, 113 (2022).
  - [6] Y. Cao, J. Romero, J. P. Olson, M. Degroote, P. D. Johnson, M. Kieferová, I. D. Kivlichan, T. Menke, B. Peropadre, N. P. D. Sawaya, S. Sim, L. Veis, and A. Aspuru-Guzik, Quantum chemistry in the age of quantum computing, *Chemical Reviews* **119**, 10856 (2019).

- [7] X. Pan, Z. Lu, W. Wang, Z. Hua, Y. Xu, W. Li, W. Cai, X. Li, H. Wang, Y.-P. Song, C.-L. Zou, D.-L. Deng, and L. Sun, Deep quantum neural networks on a superconducting processor, [Nature Communications](#) **14**, 4006 (2023).
- [8] W. Ren, W. Li, S. Xu, K. Wang, W. Jiang, F. Jin, X. Zhu, J. Chen, Z. Song, P. Zhang, H. Dong, X. Zhang, J. Deng, Y. Gao, C. Zhang, Y. Wu, B. Zhang, Q. Guo, H. Li, Z. Wang, J. Biamonte, C. Song, D.-L. Deng, and H. Wang, Experimental quantum adversarial learning with programmable superconducting qubits, [Nature Computational Science](#) **2**, 711 (2022).
- [9] H.-L. Huang, Y. Du, M. Gong, Y. Zhao, Y. Wu, C. Wang, S. Li, F. Liang, J. Lin, Y. Xu, R. Yang, T. Liu, M.-H. Hsieh, H. Deng, H. Rong, C.-Z. Peng, C.-Y. Lu, Y.-A. Chen, D. Tao, X. Zhu, and J.-W. Pan, Experimental quantum generative adversarial networks for image generation, [Phys. Rev. Appl.](#) **16**, 024051 (2021).
- [10] K. Mitarai, M. Negoro, M. Kitagawa, and K. Fujii, Quantum Circuit Learning, [Physical Review A](#) **98**, 032309 (2018), [arxiv:1803.00745](#).
- [11] A. Pérez-Salinas, A. Cervera-Lierta, E. Gil-Fuster, and J. I. Latorre, Data re-uploading for a universal quantum classifier, [Quantum](#) **4**, 226 (2020).
- [12] Y. LeCun, Y. Bengio, and G. Hinton, Deep learning, [Nature](#) **521**, 436 (2015).
- [13] A. Barron, Universal approximation bounds for superpositions of a sigmoidal function, [IEEE Transactions on Information Theory](#) **39**, 930 (1993).
- [14] D. Yarotsky, Optimal approximation of continuous functions by very deep ReLU networks, in [Proceedings of the 31st Conference On Learning Theory](#) (PMLR, 2018) pp. 639–649.
- [15] D. Yarotsky and A. Zhevnerchuk, The phase diagram of approximation rates for deep neural networks, in [Advances in Neural Information Processing Systems](#), Vol. 33 (Curran Associates, Inc., 2020) pp. 13005–13015.
- [16] P. Petersen and F. Voigtlaender, Optimal approximation of piecewise smooth functions using deep ReLU neural networks, [Neural Networks](#) **108**, 296 (2018).
- [17] Z. Shen, Deep Network Approximation Characterized by Number of Neurons, [Communications in Computational Physics](#) **28**, 1768 (2020).
- [18] J. Lu, Z. Shen, H. Yang, and S. Zhang, Deep Network Approximation for Smooth Functions, [SIAM Journal on Mathematical Analysis](#) **53**, 5465 (2021), [arxiv:2001.03040 \[cs, math, stat\]](#).
- [19] Z. Shen, H. Yang, and S. Zhang, Optimal Approximation Rate of ReLU Networks in terms of Width and Depth, [Journal de Mathématiques Pures et Appliquées](#) **157**, 101 (2022), [arxiv:2103.00502 \[cs, stat\]](#).
- [20] V. Havlíček, A. D. Córcoles, K. Temme, A. W. Harrow, A. Kandala, J. M. Chow, and J. M. Gambetta, Supervised learning with quantum-enhanced feature spaces, [Nature](#) **567**, 209 (2019).
- [21] Y. Du, M.-H. Hsieh, T. Liu, and D. Tao, Expressive power of parametrized quantum circuits, [Physical Review Research](#) **2**, 033125 (2020).
- [22] Y. Liu, S. Arunachalam, and K. Temme, A rigorous and robust quantum speed-up in supervised machine learning, [Nature Physics](#) **17**, 1013 (2021).
- [23] H.-Y. Huang, R. Kueng, and J. Preskill, Information-theoretic bounds on quantum advantage in machine learning, [Phys. Rev. Lett.](#) **126**, 190505 (2021).
- [24] S. Jerbi, C. Gyurik, S. Marshall, H. Briegel, and V. Dunjko, Parametrized Quantum Policies for Reinforcement Learning, in [Advances in Neural Information Processing Systems](#), Vol. 34 (Curran Associates, Inc., 2021) pp. 28362–28375.
- [25] H.-Y. Huang, M. Broughton, M. Mohseni, R. Babbush, S. Boixo, H. Neven, and J. R. McClean, Power of data in quantum machine learning, [Nature Communications](#) **12**, 2631 (2021).
- [26] S. Jerbi, L. J. Fiderer, H. Poulsen Nautrup, J. M. Kübler, H. J. Briegel, and V. Dunjko, Quantum machine learning beyond kernel methods, [Nature Communications](#) **14**, 517 (2023).
- [27] J. Jäger and R. V. Krems, Universal expressiveness of variational quantum classifiers and quantum kernels for support vector machines, [Nature Communications](#) **14**, 576 (2023).
- [28] F. J. Gil Vidal and D. O. Theis, Input Redundancy for Parameterized Quantum Circuits, [Frontiers in Physics](#) **8** (2020).
- [29] M. Schuld, R. Sweke, and J. J. Meyer, Effect of data encoding on the expressive power of variational quantum-machine-learning models, [Physical Review A](#) **103**, 032430 (2021).
- [30] A. Pérez-Salinas, D. López-Núñez, A. García-Sáez, P. Forn-Díaz, and J. I. Latorre, One qubit as a universal approximant, [Physical Review A](#) **104**, 012405 (2021).
- [31] Z. Yu, H. Yao, M. Li, and X. Wang, Power and limitations of single-qubit native quantum neural networks, in [Advances in Neural Information Processing Systems](#), Vol. 35, edited by S. Koyejo, S. Mohamed, A. Agarwal, D. Belgrave, K. Cho, and A. Oh (Curran Associates, Inc., 2022) pp. 27810–27823.

- [32] A. Manzano, D. Dechant, J. Tura, and V. Dunjko, [Parametrized Quantum Circuits and their approximation capacities in the context of quantum machine learning](#) (2023), [arxiv:2307.14792 \[quant-ph\]](#).
- [33] G. H. Low, T. J. Yoder, and I. L. Chuang, Methodology of Resonant Equiangular Composite Quantum Gates, [Physical Review X](#) **6**, 041067 (2016).
- [34] G. H. Low and I. L. Chuang, Optimal Hamiltonian Simulation by Quantum Signal Processing, [Physical Review Letters](#) **118**, 010501 (2017).
- [35] A. Gilyén, Y. Su, G. H. Low, and N. Wiebe, Quantum singular value transformation and beyond: Exponential improvements for quantum matrix arithmetics, in [Proceedings of the 51st Annual ACM SIGACT Symposium on Theory of Computing](#) (2019) pp. 193–204, [arxiv:1806.01838 \[quant-ph\]](#).
- [36] T. Goto, Q. H. Tran, and K. Nakajima, Universal Approximation Property of Quantum Machine Learning Models in Quantum-Enhanced Feature Spaces, [Physical Review Letters](#) **127**, 090506 (2021).
- [37] A. M. Childs and N. Wiebe, Hamiltonian simulation using linear combinations of unitary operations, [Quantum Inf. Comput.](#) **12**, 901 (2012).
- [38] A. J. da Silva and D. K. Park, Linear-depth quantum circuits for multiqubit controlled gates, [Physical Review A](#) **106**, 042602 (2022).
- [39] G. Brassard, P. Hoyer, M. Mosca, and A. Tapp, Quantum Amplitude Amplification and Estimation, [Contemporary Mathematics](#) **305**, 53 (2002).
- [40] K. R. Davidson and A. P. Donsig, [Real analysis with real applications](#) (Prentice Hall, 2002).
- [41] C. Heitzinger, [Simulation and Inverse Modeling of Semiconductor Manufacturing Processes](#), Thesis, Technische Universität Wien (2002).
- [42] M. Foupouagnigni and M. Mouafo Wouodjié, On Multivariate Bernstein Polynomials, [Mathematics](#) **8**, 1397 (2020).
- [43] Y. Jiao, G. Shen, Y. Lin, and J. Huang, [Deep Nonparametric Regression on Approximate Manifolds: Non-Asymptotic Error Bounds with Polynomial Prefactors](#) (2023), [arxiv:2104.06708 \[math, stat\]](#).
- [44] G. H. Low, [Quantum Signal Processing by Single-Qubit Dynamics](#), Thesis, Massachusetts Institute of Technology (2017).
- [45] J. Deng, W. Dong, R. Socher, L.-J. Li, K. Li, and L. Fei-Fei, ImageNet: A large-scale hierarchical image database, in [2009 IEEE Conference on Computer Vision and Pattern Recognition](#) (2009) pp. 248–255.
- [46] L. Gonon and A. Jacquier, Universal Approximation Theorem and error bounds for quantum neural networks and quantum reservoirs (2023), [arxiv:2307.12904 \[quant-ph\]](#).
- [47] Y. Wang, L. Zhang, Z. Yu, and X. Wang, Quantum Phase Processing and its Applications in Estimating Phase and Entropies (2023), [arxiv:2209.14278 \[math-ph, physics:quant-ph\]](#).
- [48] V. N. Vapnik and A. Ya. Chervonenkis, Necessary and Sufficient Conditions for the Uniform Convergence of Means to their Expectations, [Theory of Probability & Its Applications](#) **26**, 532 (1982).
- [49] V. M. Tikhomirov,  $\epsilon$ -Entropy and  $\epsilon$ -Capacity of Sets In Functional Spaces, in [Selected Works of A. N. Kolmogorov: Volume III: Information Theory and the Theory of Algorithms](#), Mathematics and Its Applications, edited by A. N. Shiriyayev (Springer Netherlands, Dordrecht, 1993) pp. 86–170.
- [50] P. L. Bartlett and S. Mendelson, Rademacher and Gaussian Complexities: Risk Bounds and Structural Results, [Journal of Machine Learning Research](#) **3**, 463 (2003).
- [51] Y. Du, Z. Tu, X. Yuan, and D. Tao, Efficient Measure for the Expressivity of Variational Quantum Algorithms, [Physical Review Letters](#) **128**, 080506 (2022).
- [52] K. Bu, D. E. Koh, L. Li, Q. Luo, and Y. Zhang, Statistical complexity of quantum circuits, [Physical Review A](#) **105**, 062431 (2022).
- [53] M. C. Caro and I. Datta, Pseudo-dimension of quantum circuits, [Quantum Machine Intelligence](#) **2**, 14 (2020).
- [54] C.-C. Chen, M. Sogabe, K. Shiba, K. Sakamoto, and T. Sogabe, General Vapnik–Chervonenkis dimension bounds for quantum circuit learning, [Journal of Physics: Complexity](#) **3**, 045007 (2022).
- [55] A. Abbas, D. Sutter, C. Zoufal, A. Lucchi, A. Figalli, and S. Woerner, The power of quantum neural networks, [Nature Computational Science](#) **1**, 403 (2021).
- [56] R. A. DeVore, R. Howard, and C. Micchelli, Optimal nonlinear approximation, [manuscripta mathematica](#) **63**, 469 (1989).
- [57] G. Cybenko, Approximation by superpositions of a sigmoidal function, [Mathematics of control, signals and systems](#) **2**, 303 (1989).
- [58] K. Hornik, Approximation capabilities of multilayer feedforward networks, [Neural networks](#) **4**, 251 (1991).
- [59] W. E. C. Ma, and L. Wu, [The Barron Space and the Flow-induced Function Spaces for Neural Network Models](#) (2021), [arxiv:1906.08039 \[cs, math, stat\]](#).

- [60] M. H. Stone, The Generalized Weierstrass Approximation Theorem, *Mathematics Magazine* **21**, 167 (1948), [3029750](#).
- [61] K. He, X. Zhang, S. Ren, and J. Sun, Deep Residual Learning for Image Recognition, in *2016 IEEE Conference on Computer Vision and Pattern Recognition (CVPR)* (2016) pp. 770–778.
- [62] S. Ren, K. He, R. Girshick, and J. Sun, Faster R-CNN: Towards real-time object detection with region proposal networks, in *Advances in Neural Information Processing Systems*, Vol. 28, edited by C. Cortes, N. Lawrence, D. Lee, M. Sugiyama, and R. Garnett (Curran Associates, Inc., 2015).
- [63] Z. Yang, Z. Dai, Y. Yang, J. Carbonell, R. R. Salakhutdinov, and Q. V. Le, XLNet: Generalized Autoregressive Pretraining for Language Understanding, in *Advances in Neural Information Processing Systems*, Vol. 32 (Curran Associates, Inc., 2019).
- [64] J. Devlin, M.-W. Chang, K. Lee, and K. Toutanova, BERT: Pre-training of Deep Bidirectional Transformers for Language Understanding, in *Proceedings of the 2019 Conference of the North American Chapter of the Association for Computational Linguistics: Human Language Technologies, Volume 1 (Long and Short Papers)* (Association for Computational Linguistics, Minneapolis, Minnesota, 2019) pp. 4171–4186.
- [65] S. Zhang, J. Lu, and H. Zhao, Deep Network Approximation: Beyond ReLU to Diverse Activation Functions (2023), [arxiv:2307.06555](#) [cs, stat].
- [66] D. Yarotsky, Error bounds for approximations with deep relu networks, *Neural Networks* **94**, 103 (2017).
- [67] I. Gühring, G. Kutyniok, and P. Petersen, Error bounds for approximations with deep relu neural networks in  $w_s, p$  norms, *Analysis and Applications* **18**, 803 (2020), <https://doi.org/10.1142/S0219530519410021>.
- [68] J. Schmidt-Hieber, Nonparametric regression using deep neural networks with ReLU activation function, *The Annals of Statistics* **48**, 1875 (2020).

# Supplementary Material

## CONTENTS

I. Introduction	1
II. Results	3
A. Framework setup	3
B. PQC approximation for continuous functions	4
C. PQC approximation for Hölder smooth functions	5
III. Discussion	7
Acknowledgment	8
References	8
A. Preliminaries	12
1. Notation	13
2. Data re-uploading PQCs	13
a. Implementing real polynomials	13
b. Implementing trigonometric polynomials	14
3. Related work in PQC approximation	15
B. Implementing multivariate polynomials using PQCs	16
1. Implementing multivariate real polynomials	16
2. Implementing multivariate trigonometric polynomials	19
C. Approximating continuous functions via PQCs	20
1. Established results of Bernstein polynomials approximation	20
2. Implement Bernstein polynomials via PQCs	22
3. PQC approximating continuous functions	23
D. Approximating smooth functions via nested PQCs	24
1. Localization via PQC	24
2. Implementing the Taylor coefficients by PQC	26
3. Implementing multivariate Taylor series by PQC	26
4. Comparison of “global” and “local” approaches in this work	29
E. Comparison with related works in classical machine learning	29

### Appendix A: Preliminaries

In this section, we will first present some essential mathematical foundations for deriving the main results of this work. Moreover, to contextualize our work within the existing literature, we conduct a comprehensive review of relevant studies in Appendix A 3.

## 1. Notation

We unify the notations throughout the whole work. The univariate polynomial ring over a field  $\mathbb{F}$  is symbolized as  $\mathbb{F}[x]$ , with the variable  $x$  representing the input. The ring of Laurent polynomial  $\mathbb{F}[x, x^{-1}]$  is an extension of the polynomial ring obtained by adding inverses of  $x$ . The collection of natural numbers is represented by the symbol  $\mathbb{N} := \{1, 2, 3, \dots\}$ , while the set of non-negative integers is denoted as  $\mathbb{N}_0 := \{0\} \cup \mathbb{N}$ . The 1-norm of a vector  $\boldsymbol{\alpha} = (\alpha_1, \alpha_2, \dots, \alpha_d)$  is denoted by  $\|\boldsymbol{\alpha}\|_1 := |\alpha_1| + |\alpha_2| + \dots + |\alpha_d|$ .

## 2. Data re-uploading PQCs

In this section, we review the concept of data re-uploading PQC and define the PQC we use in this paper. The data re-uploading PQC is a quantum circuit that consists of interleaved data encoding circuit blocks and trainable circuit blocks [11, 28]. More precisely, let  $\boldsymbol{x}$  be the input data vector and  $\boldsymbol{\theta} = (\boldsymbol{\theta}_0, \dots, \boldsymbol{\theta}_L)$  be a set of trainable parameters.  $S(\boldsymbol{x})$  is a quantum circuit that encode  $\boldsymbol{x}$  and  $V(\boldsymbol{\theta}_j)$  is a trainable quantum circuit with trainable parameter vector  $\boldsymbol{\theta}_j$ . An  $L$ -layer data re-uploading PQC can be then expressed as

$$U_{\boldsymbol{\theta}}(\boldsymbol{x}) = V(\boldsymbol{\theta}_0) \prod_{j=1}^L S(\boldsymbol{x})V(\boldsymbol{\theta}_j), \quad (\text{A.1})$$

Applying  $U_{\boldsymbol{\theta}}(\boldsymbol{x})$  to a quantum state and measuring the output states provides a way to express functions on  $\boldsymbol{x}$ . The *expressivity* of the data re-uploading PQC model can be characterized by the classes of functions that it can implement. It is common to build data encoding circuits and trainable circuits using the most prevalent Pauli rotation operators,

$$R_X(\theta) = \begin{bmatrix} \cos \frac{\theta}{2} & -i \sin \frac{\theta}{2} \\ -i \sin \frac{\theta}{2} & \cos \frac{\theta}{2} \end{bmatrix}, \quad R_Y(\theta) = \begin{bmatrix} \cos \frac{\theta}{2} & -\sin \frac{\theta}{2} \\ \sin \frac{\theta}{2} & \cos \frac{\theta}{2} \end{bmatrix}, \quad R_Z(\theta) = \begin{bmatrix} e^{-i\frac{\theta}{2}} & 0 \\ 0 & e^{i\frac{\theta}{2}} \end{bmatrix}. \quad (\text{A.2})$$

Different data encoding schemes lead to different types of data re-uploading PQCs.

In some cases, trainable parameters are also included both during the initial data encoding phase and the final processing of measurement outcomes. These PQCs are considered to have *hybrid* structures. For instance, in the models proposed by Refs. [28, 30, 46], each input data is multiplied by a specific trainable parameter and subsequently subjected to  $R_Z$  gates during the data encoding stage. In a similar vein, Refs. [36, 46] incorporate trainable weights into each measurement outcome generated by the constructed PQCs, aggregating these weighted outcomes to produce the final result. Such a structure makes it hard to investigate whether the expressive power comes from the classical or quantum part.

### a. Implementing real polynomials

We first introduce the data re-uploading PQC for implementing real univariate polynomials. We utilize the so-called *Pauli X basis encoding* [10]: The data encoding unitary is a single-qubit rotation defined as

$$S(x) := e^{i \arccos(x) X} = \begin{pmatrix} x & i\sqrt{1-x^2} \\ i\sqrt{1-x^2} & x \end{pmatrix}, \quad (\text{A.3})$$

where  $x \in [-1, 1]$  is the input data. Then interlaying the data encoding unitary  $S(x)$  with some parameterized Pauli  $Z$  rotations  $R_Z(\theta)$  gives the circuit of data re-uploading PQC for one variable as

$$U_{\boldsymbol{\theta}}(x) := R_Z(\theta_0) \prod_{j=1}^L S(x)R_Z(\theta_j), \quad (\text{A.4})$$

where  $\theta = (\theta_0, \dots, \theta_L) \in \mathbb{R}^{L+1}$  is a set of trainable parameters. The PQC in Eq. (A.4) can be used to implement polynomial transformations on input  $x$ , as shown in the following lemma.

**Lemma S1** ([35]). *There exists  $\theta \in \mathbb{R}^{L+1}$  such that*

$$U_{\theta}(x) = \begin{pmatrix} P(x) & iQ(x)\sqrt{1-x^2} \\ iQ^*(x)\sqrt{1-x^2} & P^*(x) \end{pmatrix} \quad (\text{A.5})$$

if and only if polynomials  $P, Q \in \mathbb{C}[x]$  satisfy

1.  $\deg(P) \leq L$  and  $\deg(Q) \leq L - 1$ ,
2.  $P$  has parity  $L \bmod 2$  and  $Q$  has parity  $(L - 1) \bmod 2$ <sup>2</sup>,
3.  $\forall x \in [-1, 1], |P(x)|^2 + (1 - x^2)|Q(x)|^2 = 1$ .

As shown in the above lemma, one could implement a polynomial transformation  $\text{Poly}(x)$  such that  $\text{Poly}(x) = \langle 0|U_{\theta}(x)|0\rangle = P(x)$ . Notice that the achievable polynomial  $\text{Poly}(x)$  implemented in this way is limited to  $P(x)$  for which there exists a polynomial  $Q(x)$  satisfying the conditions of Lemma S1. As the target polynomial is often real in practice, we could overcome such a limitation by defining  $\text{Poly}(x) = \langle +|U_{\theta}(x)|+\rangle = \Re(P(x)) + i\Re(Q(x))\sqrt{1-x^2}$ . Then we can achieve any real polynomials with parity  $L \bmod 2$  such that  $\deg(\text{Poly}(x)) \leq L$ , and  $|\text{Poly}(x)| \leq 1$  for all  $x \in [-1, 1]$ .

**Corollary S2** ([35]). *There exists  $\theta \in \mathbb{R}^{L+1}$  such that*

$$p(x) = \langle +|U_{\theta}(x)|+\rangle \quad (\text{A.6})$$

if and only if the real polynomial  $p(x) \in \mathbb{R}[x]$  satisfies

1.  $\deg(p(x)) \leq L$ ,
2.  $p(x)$  has parity  $L \bmod 2$ <sup>3</sup>,
3.  $\forall x \in [-1, 1], |p(x)| \leq 1$ .

**Remark S1.** *The results of PQC with Pauli  $X$  basis encoding presented here have been established in the technique of quantum signal processing [33–35], which uses interleaving signal operators and signal processing operators to transform the input signal. The circuit of QSP could be identified as a PQC in the context of quantum machine learning.*

#### b. Implementing trigonometric polynomials

Other than the real polynomials, there are also types of single-qubit PQC with Pauli  $Z$  basis encoding that could implement complex trigonometric polynomials [31]. The data encoding unitary is a single-qubit rotation in the Pauli  $Z$  basis

$$S(x) := R_Z(x) = \begin{pmatrix} e^{ix/2} & 0 \\ 0 & e^{-ix/2} \end{pmatrix}, \quad (\text{A.7})$$

<sup>2</sup> For a polynomial  $P \in \mathbb{C}[x]$ ,  $P$  has parity 0 if all coefficients corresponding to odd powers of  $x$  are 0, and similarly  $P$  has parity 1 if all coefficients corresponding to even powers of  $x$  are 0.

<sup>3</sup> A polynomial  $p(x)$  has parity 0 if all coefficients corresponding to odd powers of  $x$  are 0, and similarly  $p(x)$  has parity 1 if all coefficients corresponding to even powers of  $x$  are 0.

where  $x \in \mathbb{R}$  is the data. By interleaving the data encoding unitary  $S(x)$  with trainable gates  $R_Y(\theta)R_Z(\phi)$ , the PQC is defined as

$$U_{\boldsymbol{\theta}, \boldsymbol{\phi}}(x) := R_Z(\omega)R_Y(\theta_0)R_Z(\phi_0) \prod_{j=1}^L S(x)R_Y(\theta_j)R_Z(\phi_j), \quad (\text{A.8})$$

where  $\boldsymbol{\theta} = (\theta_0, \dots, \theta_L) \in \mathbb{R}^{L+1}$ ,  $\boldsymbol{\phi} = (\phi_0, \dots, \phi_L) \in \mathbb{R}^{L+1}$  and  $\omega \in \mathbb{R}$ . The following lemma characterizes the correspondence between PQC with  $\sigma_z$  basis encoding and complex trigonometric polynomials.

**Lemma S3** ([31]). *There exist  $\boldsymbol{\theta}, \boldsymbol{\phi} \in \mathbb{R}^{L+1}$  and  $\omega \in \mathbb{R}$  such that*

$$U_{\boldsymbol{\theta}, \boldsymbol{\phi}}(x) = \begin{pmatrix} P(x) & -Q(x) \\ Q^*(x) & P^*(x) \end{pmatrix} \quad (\text{A.9})$$

if and only if Laurent polynomials  $P, Q \in \mathbb{C}[e^{ix/2}, e^{-ix/2}]$  satisfy

1.  $\deg(P) \leq L$  and  $\deg(Q) \leq L$ ,
2.  $P$  and  $Q$  have parity  $L \bmod 2$ ,
3.  $\forall x \in \mathbb{R}, |P(x)|^2 + |Q(x)|^2 = 1$ .

Note that Laurent polynomials in  $\mathbb{C}[e^{ix/2}, e^{-ix/2}]$  with parity 0 are Laurent polynomials in  $\mathbb{C}[e^{ix}, e^{-ix}]$  without parity constraints, which implies that the trigonometric QSP could implement complex trigonometric polynomials.

**Corollary S4** ([31, 47]). *There exist  $\boldsymbol{\theta}, \boldsymbol{\phi} \in \mathbb{R}^{2L+1}$  and  $\omega \in \mathbb{R}$  such that*

$$t(x) = \langle 0 | U_{\boldsymbol{\theta}, \boldsymbol{\phi}}(x) | 0 \rangle \quad (\text{A.10})$$

if and only if the complex-valued trigonometric polynomial  $t(x) = \sum_{j=-L}^L c_j e^{ijx}$  satisfies  $|t(x)| \leq 1$  for all  $x \in \mathbb{R}$ .

### 3. Related work in PQC approximation

In this subsection, we review prior literature related to the approximation capabilities of PQCs, which characterizes how the architectural properties of a PQC affect the resulting functions it can fit, and its ensuing performance. After a systematic comparison, we conclude that our results provide precise error bounds for continuous function approximation and make no assumptions about the constructed PQCs. More importantly, all the variables in our proposal take the form of parameters within rotation gates and remain distinct from the data encoding gates to avoid any classical computational influence, thus preserving the inherent quantum property of our approach.

In theoretical machine learning, statistical complexity is a notion that measures the inherent richness characterizing a given hypothesis space. There are various statistical complexity measures, including the Vapnik-Chervonenkis (VC) dimension [48], the metric entropy [49], the Gaussian complexity [50], and the Rademacher complexity [50], etc. To gauge the statistical complexity of PQCs, Du *et al.* [51] have explored the covering entropy of PQCs in terms of the number of quantum gates and the measurement observable. Bu *et al.* [52] have investigated the dependence of the Rademacher complexity of PQCs on the resources, width, depth, and the property of input and output registers. The assessment of PQCs has extended to encompass an array of statistical complexity measures, including the Pseudo-Dimension, as delineated in Caro and Datta [53], and the VC dimension, as expounded upon in Chen *et al.* [54]. Furthermore, the evaluation

of PQC expressivity has extended its purview to metrics rooted in information theory. Abbas *et al.* [55] have embarked upon an evaluation of PQC expressivity through the prism of the effective dimension, a data-dependent metric contingent upon the Fisher information. In a parallel endeavor, Du *et al.* [21] have concentrated their attention on generative tasks, employing entanglement entropy as a metric for quantifying PQC expressivity. It is important to underscore that, while statistical complexity metrics and information-inspired metrics provide invaluable insights into the ‘volume’ of hypothesis spaces, they do not furnish a precise delineation of the functions amenable to representation by these models.

To further explore the intricacies of PQCs and their expressivity, an alternative avenue of research has emerged, as highlighted by recent studies [28–32]. They rewrote the PQC output, i.e., the inner product between an input quantum state and a variational observable, in the form of partial Fourier series. This innovative perspective introduces a more nuanced toolbox for assessing PQC expressivity, offering fresh insights within the quantum machine learning domain, notably with respect to the universal approximation property (UAP). However, it is imperative to underscore that many investigations employing Fourier expansion have been predicated upon certain impractical assumptions. These assumptions encompass the demand for arbitrary parameterized global unitaries and observables, thus posing significant challenges to the practical implementation of the constructed quantum circuits. The existence proof of universal approximation also does not explicitly give approximation error bounds of PQCs.

A very general approach to expressiveness in the context of approximation is the method of nonlinear widths by DeVore *et al.* [56] that concerns the approximation of a family of functions under the assumption of a continuous dependence of the model on the approximated function. Pérez-Salinas *et al.* [30] have proved that single-qubit data re-uploading PQCs are universal function approximators, inheriting the famous universal approximation theorem for neural networks [57, 58]. In a quantum-enhanced context, Goto *et al.* [36] have constructed PQCs to approximate any continuous function guided by the Stone-Weierstrass theorem. Furthermore, Gonon and Jacquier [46] have defined a specific hypothesis space consisting of non-oscillating functions, drawing inspiration from Barron [13] and devised PQCs for approximating such functions without encountering the curse of dimensionality (CoD). Notably, the mitigation of CoD arises from their specific hypothesis space definition and is also observed within the domain of classical neural network [59]. It is essential to acknowledge that these works unveil a hybrid nature, blurring the boundaries between classical and quantum domains in circuit construction. The hybrid structure manifests in the data encoding phase and becomes evident in the weighted summation of outputs from foundational quantum circuits. Consequently, it is unclear whether the powerful expressivity comes from the classical part or the quantum part of hybrid models.

In our present work, we make no assumptions in the construction of the PQCs. In our PQC model, all variables take the form of parameters within rotation gates. Besides, these trainable parameters remain distinct from the data encoding gates to avoid any classical computational influence. These properties ensure that our constructed PQCs retain practicality and remain firmly rooted within the quantum domain.

## Appendix B: Implementing multivariate polynomials using PQCs

### 1. Implementing multivariate real polynomials

A multivariate polynomial with  $d$  variables and degree  $s \in \mathbb{N}$  is defined as

$$p(\mathbf{x}) := \sum_{\|\alpha\|_1 \leq s} c_{\alpha} \mathbf{x}^{\alpha}, \quad (\text{B.1})$$

where  $\mathbf{x} = (x_1, \dots, x_d) \in \mathbb{R}^d$ ,  $\alpha = (\alpha_1, \dots, \alpha_d) \in \mathbb{N}^d$ ,  $c_{\alpha} \in \mathbb{R}$  and  $\mathbf{x}^{\alpha} = x_1^{\alpha_1} x_2^{\alpha_2} \dots x_d^{\alpha_d}$ . To implement the multivariate polynomial  $p(\mathbf{x})$ , we first build a PQC to express a monomial  $c_{\alpha} \mathbf{x}^{\alpha} = c_{\alpha} x_1^{\alpha_1} x_2^{\alpha_2} \dots x_d^{\alpha_d}$ ,

where  $|c_\alpha \mathbf{x}^\alpha| \leq 1$  for  $\mathbf{x} \in [0, 1]^d$  and  $\|\alpha\|_1 \leq s$ . We apply the single-qubit PQC with Pauli  $X$  basis encoding defined in Eq. (A.4) on each  $x_j$  for  $1 \leq j \leq d$ , respectively.

**Lemma S5.** *Given a monomial  $c_\alpha \mathbf{x}^\alpha = c_\alpha x_1^{\alpha_1} x_2^{\alpha_2} \cdots x_d^{\alpha_d}$  such that  $|c_\alpha \mathbf{x}^\alpha| \leq 1$  for all  $\mathbf{x} \in [0, 1]^d$  and  $\|\alpha\|_1 \leq s$  for  $s \in \mathbb{N}$ , there exists a PQC  $U^\alpha(\mathbf{x})$  such that*

$$\langle + |^{\otimes d} U^\alpha(\mathbf{x}) | + \rangle^{\otimes d} = c_\alpha \mathbf{x}^\alpha. \quad (\text{B.2})$$

The width of the PQC is at most  $d$ , the depth is at most  $2s + 1$ , and the number of parameters is at most  $s + d$ .

*Proof.* By Corollary S2, there exist  $d$  single-qubit PQCs  $U_{\theta_1}^{\alpha_1}(x_1), U_{\theta_2}^{\alpha_2}(x_2), \dots, U_{\theta_d}^{\alpha_d}(x_d)$  such that

$$\begin{aligned} \langle + | U_{\theta_1}^{\alpha_1}(x_1) | + \rangle &= c_\alpha x_1^{\alpha_1}, \\ \langle + | U_{\theta_2}^{\alpha_2}(x_2) | + \rangle &= x_2^{\alpha_2}, \\ &\dots \\ \langle + | U_{\theta_d}^{\alpha_d}(x_d) | + \rangle &= x_d^{\alpha_d}, \end{aligned}$$

where the number of layers of each PQC is  $L_j = \alpha_j$  for  $1 \leq j \leq d$ . We then define a  $d$ -qubit PQC as

$$U^\alpha(\mathbf{x}) = \bigotimes_{j=1}^d U_{\theta_j}^{\alpha_j}(x_j), \quad (\text{B.3})$$

which gives

$$\langle + |^{\otimes d} U^\alpha(\mathbf{x}) | + \rangle^{\otimes d} = \prod_{j=1}^d \langle + | U_{\theta_j}^{\alpha_j}(x_j) | + \rangle = c_\alpha \mathbf{x}^\alpha. \quad (\text{B.4})$$

Since  $\|\alpha\|_1 = \sum_{j=1}^d \alpha_j \leq s$ , we can conclude that the depth of  $U^\alpha(\mathbf{x})$  is at most  $2s + 1$  and the number of parameters in  $U^\alpha(\mathbf{x})$  is at most  $s + d$ .  $\square$

The next step is to combine monomials together to implement the multivariate polynomial. Specifically, we would like to implement the following (unnormalized) operator

$$U_p(\mathbf{x}) := \sum_{\|\alpha\|_1 \leq s} U^\alpha(\mathbf{x}) \quad (\text{B.5})$$

so that we can implement an (unnormalized) polynomial as

$$\langle + |^{\otimes d} U_p(\mathbf{x}) | + \rangle^{\otimes d} = \sum_{\|\alpha\|_1 \leq s} \langle + |^{\otimes d} U^\alpha(\mathbf{x}) | + \rangle^{\otimes d} = \sum_{\|\alpha\|_1 \leq s} c_\alpha \mathbf{x}^\alpha = p(\mathbf{x}). \quad (\text{B.6})$$

We denote  $T$  the number of terms in the summation and observe that it can be bounded as

$$T = \sum_{\|\alpha\|_1 \leq s} 1 = \sum_{j=0}^s \sum_{\|\alpha\|_1=j} 1 \leq \sum_{j=0}^s d^j \leq (s+1)d^s. \quad (\text{B.7})$$

For convenience, we rewrite the normalized target operator with  $\alpha$  being an indexed variable as

$$U_p(\mathbf{x}) = \sum_{j=1}^T \frac{1}{T} U^{\alpha^{(j)}}(\mathbf{x}). \quad (\text{B.8})$$

However, the addition operation in quantum computing is non-trivial as the sum of unitary operators is not necessarily unitary. To sum the monomials together, we utilize the technique of *linear combination of unitaries* (LCU) [37] to implement the operator  $U_p(\mathbf{x})$  in Eq. (B.8) on a quantum computer. We first construct a unitary operator  $F$  such that

$$F|0\rangle = \frac{1}{\sqrt{T}} \sum_{j=1}^T |j\rangle. \quad (\text{B.9})$$

The unitary  $F$  could be simply implemented by Hadamard gates. Next, we construct a controlled unitary

$$U_c(\mathbf{x}) = \sum_{j=1}^T |j\rangle\langle j| \otimes U^{\alpha^{(j)}}(\mathbf{x}). \quad (\text{B.10})$$

Note that each  $|j\rangle\langle j| \otimes U^{\alpha^{(j)}}(\mathbf{x})$  could be constructed using  $(\log T)$ -qubit controlled Pauli rotation gates, as  $U^{\alpha^{(j)}}(\mathbf{x})$  consisting of single-qubit Pauli rotation gates. The  $(\log T)$ -qubit controlled gates could be further decomposed into quantum circuits of CNOT gates and single-qubit rotation gates in  $O(\log T)$  circuit depth, without using any ancilla qubit. We refer to the detailed implementation of these multi-controlled gates to da Silva and Park [38]. Then the unitary  $W_{lcu} = (F^\dagger \otimes I)U_c(F \otimes I)$  satisfies that

$$W_{lcu}|0\rangle|+\rangle^{\otimes d} = |0\rangle U_p(\mathbf{x})|+\rangle^{\otimes d} + |\perp\rangle, \quad (\text{B.11})$$

where  $\langle 0| \otimes I |\perp\rangle = 0$ . Notice that

$$\langle 0| \langle +|^{\otimes d} W_{lcu} |0\rangle |+\rangle^{\otimes d} = \langle +|^{\otimes d} U_p(\mathbf{x}) |+\rangle^{\otimes d} = p(\mathbf{x}). \quad (\text{B.12})$$

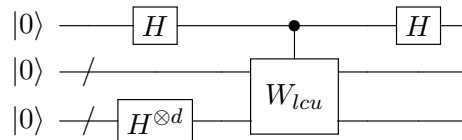
To obtain the polynomial  $p(\mathbf{x})$ , we could estimate  $\langle 0| \langle +|^{\otimes d} W_{lcu} |0\rangle |+\rangle^{\otimes d}$  using the Hadamard test.

**Proposition 1.** *For any multivariate polynomial  $p(\mathbf{x})$  with  $d$  variables and degree  $s$  such that  $|p(\mathbf{x})| \leq 1$  for  $\mathbf{x} \in [0, 1]^d$ , there exists a PQC  $W_p(\mathbf{x})$  such that*

$$f_{W_p}(\mathbf{x}) := \langle 0| W_p^\dagger(\mathbf{x}) Z^{(0)} W_p(\mathbf{x}) |0\rangle = p(\mathbf{x}) \quad (\text{B.13})$$

where  $Z^{(0)}$  is the Pauli  $Z$  observable on the first qubit. The width of the PQC is  $O(d + \log s + s \log d)$ , the depth is  $O(s^2 d^s (\log s + s \log d))$ , and the number of parameters is  $O(sd^s(s + d))$ .

*Proof.* We apply the Hadamard test on  $W_{lcu}$ , giving the quantum circuit  $W_p(\mathbf{x})$  as follows.



Measuring the first qubit of  $W_p(\mathbf{x})$ , we have

$$f_{W_p}(\mathbf{x}) := \langle 0| W_p^\dagger(\mathbf{x}) Z^{(0)} W_p(\mathbf{x}) |0\rangle = \langle 0| \langle +|^{\otimes d} W_{lcu} |0\rangle |+\rangle^{\otimes d} = p(\mathbf{x}). \quad (\text{B.14})$$

The controlled unitary used in LCU,

$$U_c(\mathbf{x}) = \sum_{j=1}^T |j\rangle\langle j| \otimes U^{\alpha^{(j)}}(\mathbf{x}), \quad (\text{B.15})$$

could be implemented by at most  $O(Ts)$   $(\log T)$ -qubit controlled gates. A  $(\log T)$ -qubit controlled gate could be implemented by a quantum circuit consisting of CNOT gates and single-qubit gates with depth  $O(\log T)$  [38]. Thus  $U_c(\mathbf{x})$  could be implemented by a quantum circuit with depth  $O(sT \log T)$  and width  $O(d + \log T)$ . Then the depth and width of  $W_{icu} = (F^\dagger \otimes I)U_c(F \otimes I)$  are in the same order of  $U_c(\mathbf{x})$  since  $F$  is simply tensor of Hadamard gates. Therefore the entire depth of the circuit  $W_p$  is  $O(sT \log T + d)$  and the width of  $W_p$  is  $O(d + \log T)$ . As  $T \leq (s+1)d^s$ . Note that the number of parameters in the PQC equals the number of parameters in  $U_c(\mathbf{x})$ , which is  $O(T(s+d))$ .  $\square$

Note that measuring the first qubit of  $W_p(\mathbf{x})$  for  $O(\frac{1}{\varepsilon})$  times is needed to estimate the value of  $p(\mathbf{x})$  up to an additive error  $\varepsilon$ . We could further use the amplitude estimation algorithm [39] to reduce the overhead while increasing the circuit depth by  $O(\frac{1}{\varepsilon})$ .

## 2. Implementing multivariate trigonometric polynomials

Here we extend the PQCs with  $R_Z$  encoding to implement multivariate trigonometric polynomials. A multivariate trigonometric polynomials with  $d$  variables and degree  $s$  is defined as

$$t(\mathbf{x}) := \sum_{\|\mathbf{n}\|_1 \leq s} c_{\mathbf{n}} e^{i\mathbf{n} \cdot \mathbf{x}} \quad (\text{B.16})$$

where  $c_{\mathbf{n}} \in \mathbb{C}$ ,  $\mathbf{x} = (x_1, \dots, x_d) \in \mathbb{R}^d$ ,  $\mathbf{v} = (\alpha_1, \dots, \alpha_d) \in \mathbb{Z}^d$ , and  $e^{i\mathbf{n} \cdot \mathbf{x}} = e^{in_1 x_1} e^{in_2 x_2} \dots e^{in_d x_d}$ . Consider a trigonometric monomial  $c_{\mathbf{n}} e^{i\mathbf{n} \cdot \mathbf{x}} = c_{\mathbf{n}} e^{in_1 x_1} e^{in_2 x_2} \dots e^{in_d x_d}$  such that  $|c_{\mathbf{n}} e^{i\mathbf{n} \cdot \mathbf{x}}| \leq 1$  for all  $\mathbf{x} \in \mathbb{R}^d$  and  $\|\mathbf{n}\|_1 \leq s$ , we could apply the single-qubit PQC with  $R_Z$  encoding as defined in Eq. (A.8) on each  $x_j$  for  $1 \leq j \leq d$  respectively.

**Lemma S6.** *Given a trigonometric monomial  $c_{\mathbf{n}} e^{i\mathbf{n} \cdot \mathbf{x}} = c_{\mathbf{n}} e^{in_1 x_1} e^{in_2 x_2} \dots e^{in_d x_d}$  such that  $|c_{\mathbf{n}} e^{i\mathbf{n} \cdot \mathbf{x}}| \leq 1$  for all  $\mathbf{x} \in \mathbb{R}^d$  and  $\|\mathbf{n}\|_1 \leq s$ , there exists a PQC  $U^{\mathbf{n}}(\mathbf{x})$  such that*

$$\langle 0 |^{\otimes d} U^{\mathbf{n}}(\mathbf{x}) | 0 \rangle^{\otimes d} = c_{\mathbf{n}} e^{i\mathbf{n} \cdot \mathbf{x}}. \quad (\text{B.17})$$

The width of the PQC is at most  $d$ , the depth is at most  $6s + 3$ , and the number of parameters is at most  $4s + 3d$ .

*Proof.* By Corollary S4, we could construct  $d$  single-qubit PQCs  $U_{\theta_1, \phi_1}^{n_1}(x_1), U_{\theta_2, \phi_2}^{n_2}(x_2), \dots, U_{\theta_d, \phi_d}^{n_d}(x_d)$  such that

$$\begin{aligned} \langle 0 | U_{\theta_1, \phi_1}^{n_1}(x_1) | 0 \rangle &= c_{\mathbf{n}} e^{in_1 x_1}, \\ \langle 0 | U_{\theta_2, \phi_2}^{n_2}(x_2) | 0 \rangle &= e^{in_2 x_2}, \\ &\dots \\ \langle 0 | U_{\theta_d, \phi_d}^{n_d}(x_d) | 0 \rangle &= e^{in_d x_d}, \end{aligned}$$

where the number of layers of each PQC is  $L_j = n_j$  for  $1 \leq j \leq d$ . We then define a  $d$ -qubit PQC as

$$U^{\mathbf{n}}(\mathbf{x}) = \bigotimes_{j=1}^d U_{\theta_j, \phi_j}^{n_j}(x_j), \quad (\text{B.18})$$

which gives

$$\langle 0 |^{\otimes d} U^{\mathbf{n}}(\mathbf{x}) | 0 \rangle^{\otimes d} = \prod_{j=1}^d \langle 0 | U_{\theta_j, \phi_j}^{n_j}(x_j) | 0 \rangle = c_{\mathbf{n}} e^{i\mathbf{n} \cdot \mathbf{x}}. \quad (\text{B.19})$$

Since  $\|\mathbf{n}\|_1 = \sum_{j=1}^d n_j \leq s$ , we can conclude that the depth of  $U^{\mathbf{n}}(\mathbf{x})$  is at most  $6s + 3$  and the number of parameters in  $U^{\mathbf{n}}(\mathbf{x})$  is at most  $4s + 3d$ .  $\square$

Then we could apply the technique of LCU on the PQC's  $U^n(\mathbf{x})$  to implement the operator

$$U_t(\mathbf{x}) := \sum_{\|\mathbf{n}\|_1 \leq s} U^n(\mathbf{x}), \quad (\text{B.20})$$

so that we can implement the multivariate trigonometric polynomial as

$$\langle + |^{\otimes d} U_t(\mathbf{x}) | + \rangle^{\otimes d} = \sum_{\|\mathbf{n}\|_1 \leq s} \langle + |^{\otimes d} U^n(\mathbf{x}) | + \rangle^{\otimes d} = \sum_{\|\mathbf{n}\|_1 \leq s} c_{\mathbf{n}} e^{i\mathbf{n} \cdot \mathbf{x}} = t(\mathbf{x}). \quad (\text{B.21})$$

Note that the number of terms in the summation is

$$\sum_{\|\mathbf{n}\|_1 \leq s} 1 = \sum_{j=0}^s \sum_{\|\mathbf{n}\|_1=j} 1 \leq \sum_{j=0}^s d^{2j} \leq (s+1)d^{2s}. \quad (\text{B.22})$$

Then we have the following proposition.

**Proposition S7.** *For any multivariate trigonometric polynomial  $t(\mathbf{x})$  with  $d$  variables and degree  $s$  such that  $|t(\mathbf{x})| \leq 1$  for  $\mathbf{x} \in \mathbb{R}^d$ , there exists a PQC  $W_{tri}(\mathbf{x})$  such that*

$$f_{W_{tri}}(\mathbf{x}) := \langle 0 | W_{tri}^\dagger(\mathbf{x}) Z^{(0)} W_{tri}(\mathbf{x}) | 0 \rangle = t(\mathbf{x}) \quad (\text{B.23})$$

where  $Z^{(0)}$  is the Pauli  $Z$  observable on the first qubit. The width of the PQC is  $O(d + \log s + s \log d)$ , the depth is  $O(s^2 d^{2s} (\log s + s \log d))$ , and the number of parameters is  $O(sd^{2s}(s+d))$ .

The proof is similar to Proposition 1. This result demonstrates the universal approximation property of PQC in the perspective of multivariate Fourier series, which yields similar results as in Schuld *et al.* [29]. Notably, the PQC in Proposition S7 has an explicit construction without any assumption, improving the implicit PQC's proposed in Schuld *et al.* [29] in terms of circuit size. For instance, to implement the  $d$ -variable Fourier series with degree  $s$ , the PQC with parallel structure in Schuld *et al.* [29] requires width  $O(ds)$  and potentially exponential depth  $O(4^{ds})$ .

### Appendix C: Approximating continuous functions via PQCs

We have constructively shown that PQCs could implement multivariate polynomials in the previous section. To study the approximation capabilities of PQC, a natural strategy involves aggregating multiple polynomials to approximate the continuous function, drawing on well-established principles from classical approximation theory. In the context of univariate functions, this endeavor is guided by the Stone-Weierstrass Theorem [60]. For the multivariate case, we accomplish this task by employing PQCs to implement Bernstein polynomials, followed by the established result on the approximation error bound of Bernstein polynomials [41, 42].

#### 1. Established results of Bernstein polynomials approximation

For a  $d$ -variable continuous function  $f : \mathbb{R}^d \rightarrow \mathbb{R}$ , the multivariate Bernstein polynomial with degree  $n \in \mathbb{N}$  of  $f$  is defined as

$$B_n(f; \mathbf{x}) := \sum_{k_1=0}^n \cdots \sum_{k_d=0}^n f\left(\frac{\mathbf{k}}{n}\right) \prod_{j=1}^d \binom{n}{k_j} x_j^{k_j} (1-x_j)^{n-k_j}, \quad (\text{C.1})$$

and  $\mathbf{k} = (k_1, \dots, k_d) \in \{0, \dots, n\}^d$ . Then we have the following lemma on the approximation error bound of the Bernstein polynomial.

**Lemma S8** (Bernstein polynomials approximation for Lipschitz functions [42]). *Given a Lipschitz continuous function  $f : [0, 1]^d \rightarrow \mathbb{R}$  with Lipschitz constant  $\ell$ , which is defined as  $|f(\mathbf{x}) - f(\mathbf{y})| \leq \ell \|\mathbf{x} - \mathbf{y}\|_\infty$ . Let  $f$  be bounded by  $\Gamma$ . The approximation error of the  $n$ -degree Bernstein polynomial of  $f$  scales as*

$$|f(\mathbf{x}) - B_n(f; \mathbf{x})| \leq \varepsilon + 2\Gamma \sum_{j=1}^d \binom{d}{j} \left(\frac{\ell^2}{4n\varepsilon^2}\right)^j \leq \varepsilon + 2\Gamma \left( \left(1 + \frac{\ell^2}{4n\varepsilon^2}\right)^d - 1 \right), \quad (\text{C.2})$$

where  $\varepsilon > 0$  is an arbitrarily small quantity.

*Proof.* Drawing inspiration from the Lipschitz continuity of the target function  $f$ , we define  $\delta = \varepsilon/\ell$ . Consequently, for any two points  $\mathbf{x} = (x_1, \dots, x_d)$  and  $\mathbf{y} = (y_1, \dots, y_d)$  such that  $|x_i - y_i| < \delta$  for all  $i \in \{1, \dots, d\}$ , it follows that  $|f(\mathbf{x}) - f(\mathbf{y})| \leq \varepsilon$ . The target function can be written as

$$\begin{aligned} f(\mathbf{x}) &= f(x_1, \dots, x_d) \\ &= f(x_1, \dots, x_d) \sum_{k_1=0}^n \cdots \sum_{k_d=0}^n \prod_{i=1}^d \binom{n}{k_i} x_i^{k_i} (1-x_i)^{n-k_i} \\ &= \sum_{k_1=0}^n \cdots \sum_{k_d=0}^n f(x_1, \dots, x_d) \prod_{i=1}^d \binom{n}{k_i} x_i^{k_i} (1-x_i)^{n-k_i}. \end{aligned} \quad (\text{C.3})$$

Let us consider the set  $E = \prod_{i=1}^d \{0, 1, \dots, n\}$ , and for  $j = 1, 2, \dots, d$ , we define the sets

$$\Omega_j = \{k_j \in \{0, 1, \dots, n\} : \left| \frac{k_j}{n} - x_j \right| < \delta\} \text{ and } F = E \setminus (\Omega_1 \times \cdots \times \Omega_d). \quad (\text{C.4})$$

Then,  $F = \bigcup_{k=1}^d F_k$ , with  $F_k = \left\{ \prod_{i=1}^d \Omega_{ik}^{\alpha_{ik}} \in F : \alpha_{ik} \in \{0, 1\}, \sum_{i=1}^d \alpha_{ik} = k \right\}$ , where  $\Omega_{ik}^{\alpha_{ik}} = \begin{cases} \Omega_i & \text{if } \alpha_{ik} = 0 \\ \Omega_i^c & \text{if } \alpha_{ik} = 1 \end{cases}$  and  $\Omega_i^c = \left\{ k_i \in \{0, \dots, n\} : \left| \frac{k_i}{n} - x_i \right| \geq \delta \right\}$ . For  $A_k = \prod_{i=1}^d \Omega_{ik}^{\alpha_{ik}} \in F_k, k = 1, \dots, d$ , let us define also  $I_{A_k} = \{i \in \{1, \dots, d\} : \alpha_{ik} = 1\}$  (that means  $\text{card}(I_{A_k}) = k \geq 1$ ). We have

$$\begin{aligned} &|f(x_1, \dots, x_d) - B_n(f; x_1, \dots, x_d)| \\ &= \left| \sum_{k_1=0}^n \cdots \sum_{k_d=0}^n f(x_1, \dots, x_d) \prod_{i=1}^d \binom{n}{k_i} x_i^{k_i} (1-x_i)^{n-k_i} \right. \\ &\quad \left. - \sum_{k_1=0}^n \cdots \sum_{k_d=0}^n f\left(\frac{k_1}{n}, \dots, \frac{k_d}{n}\right) \prod_{i=1}^d \binom{n}{k_i} x_i^{k_i} (1-x_i)^{n-k_i} \right| \\ &= \left| \sum_{k_1=0}^n \cdots \sum_{k_d=0}^n \left[ f(x_1, \dots, x_d) - f\left(\frac{k_1}{n}, \dots, \frac{k_d}{n}\right) \right] \prod_{i=1}^d \binom{n}{k_i} x_i^{k_i} (1-x_i)^{n-k_i} \right| \\ &\leq \sum_{k_1=0}^n \cdots \sum_{k_d=0}^n \left| f(x_1, \dots, x_d) - f\left(\frac{k_1}{n}, \dots, \frac{k_d}{n}\right) \right| \prod_{i=1}^d \binom{n}{k_i} x_i^{k_i} (1-x_i)^{n-k_i} \\ &\leq \sum_{\Omega_1} \cdots \sum_{\Omega_d} \left| f(x_1, \dots, x_d) - f\left(\frac{k_1}{n}, \dots, \frac{k_d}{n}\right) \right| \prod_{i=1}^d \binom{n}{k_i} x_i^{k_i} (1-x_i)^{n-k_i} \\ &\quad + \sum_F \left| f(x_1, \dots, x_d) - f\left(\frac{k_1}{n}, \dots, \frac{k_d}{n}\right) \right| \prod_{i=1}^d \binom{n}{k_i} x_i^{k_i} (1-x_i)^{n-k_i}. \end{aligned} \quad (\text{C.5})$$

Using the fact that  $f$  is continuous and bounded, we get

$$\begin{aligned}
& |f(x_1, \dots, x_d) - B_n(f; x_1, \dots, x_d)| \\
& \leq \varepsilon \sum_{\Omega_1} \dots \sum_{\Omega_d} \prod_{i=1}^d \binom{n}{k_i} x_i^{k_i} (1-x_i)^{n-k_i} + 2\Gamma \sum_F \prod_{i=1}^d \binom{n}{k_i} x_i^{k_i} (1-x_i)^{n-k_i} \\
& \leq \varepsilon + 2\Gamma \sum_{l=1}^d \sum_{A_l \in F_l} \prod_{i=1}^d \binom{n}{k_i} x_i^{k_i} (1-x_i)^{n-k_i} \\
& \leq \varepsilon + 2\Gamma \sum_{l=1}^d \sum_{A_l \in F_l} \prod_{i \in I_{A_l}} \frac{1}{4n\delta^2} \\
& = \varepsilon + 2\Gamma \sum_{j=1}^d \binom{d}{j} \frac{1}{(4n\delta^2)^j} \leq \varepsilon + 2\Gamma \left( \left(1 + \frac{\ell^2}{4n\varepsilon^2}\right)^d - 1 \right).
\end{aligned} \tag{C.6}$$

This completes the proof. A more detailed expansion of Eq. (C.6) can be seen in Theorem 2 in Foupouagnigni and Mouafo Wouodjié [42].  $\square$

**Remark S2.** Here, it is important to observe that for a continuous target function, denoted as  $f(\mathbf{x})$ , there exists a value of  $\delta > 0$  such that:

$$|f(x_1, \dots, x_d) - B_n(f; x_1, \dots, x_d)| \leq \varepsilon + 2\Gamma \left( \left(1 + \frac{1}{4n\delta^2}\right)^d - 1 \right).$$

This expression signifies the convergence rate of the Bernstein polynomial for general continuous functions.

## 2. Implement Bernstein polynomials via PQCs

In Lemma S8, we have defined the Bernstein polynomial and its approximation error towards the Lipschitz continuous function. Guided by Proposition 1, we can construct a PQC to implement such a Bernstein polynomial.

**Lemma S9.** For any  $d$ -variable Bernstein polynomial with degree  $n \in \mathbb{N}$  defined in Eq. (C.1) such that  $|B_n(f; \mathbf{x})| \leq 1$  for  $\mathbf{x} \in [0, 1]^d$ , there exist a PQC  $W_b(\mathbf{x})$  satisfying

$$f_{W_b}(\mathbf{x}) := \langle 0 | W_b^\dagger(\mathbf{x}) Z^{(0)} W_b(\mathbf{x}) | 0 \rangle = B_n(f; \mathbf{x}). \tag{C.7}$$

The width of the PQC is  $O(d \log n)$ , the depth is  $O(dn^d \log n)$ , and the number of parameters is  $O(dn^d)$ .

*Proof.* In the proof of Lemma S9, we undertake a two-step process. Initially, we construct PQCs to provide an exact representation of  $f\left(\frac{\mathbf{k}}{n}\right) \prod_{j=1}^d \binom{n}{k_j} x_j^{k_j} (1-x_j)^{n-k_j}$  for all  $\mathbf{k} \in \{0, 1, \dots, n\}^d$ . Subsequently, we employ the LCU technology to aggregate these PQCs for the purpose of approximating the Bernstein polynomial described in Eq. (C.1).

The univariate polynomial  $x^k(1-x)^{n-k}$  can be represented by a PQC. The depth of this PQC is less than  $2n + 1$ , the width is 2, the number of parameters is  $n + 2$ . The multivariate polynomial  $f\left(\frac{\mathbf{k}}{n}\right) \prod_{j=1}^d \binom{n}{k_j} x_j^{k_j} (1-x_j)^{n-k_j}$  can be exactly represented by the product of the univariate polynomial  $x^k(1-x)^{n-k}$ . The same routine has been employed in Lemma S5. The depth of this PQC is less than  $2n + 1$ , the width is  $2d$ , and the number of parameters is  $d(n + 2)$ .

The number of terms in the summation in Eq. (C.1) is  $(n+1)^d$ . We can employ the same routine in Proposition 1 to construct the PQC  $W_b(\mathbf{x})$ . The depth of  $W_b$  scales as

$$O\left((d(n+1)^{d+1} \log(n+1) + d)\right),$$

the width is  $2d + d \log(n+1)$ , and the number of parameters is  $(n+1)^d(n+2)d$ . The results presented in Lemma S9 can be obtained after simplification.  $\square$

### 3. PQC approximating continuous functions

We have successfully derived results regarding the approximation error between PQCs and Bernstein polynomials, as well as between Bernstein polynomials and continuous functions. Leveraging these established findings, we can now formulate a rigorous assertion regarding the universal approximation theorem and the error bound of PQCs, employing the well-established principles of triangle inequality.

**Theorem 1** (The Universal Approximation Theorem of PQC). *For any continuous function  $f : [0, 1]^d \rightarrow [-1, 1]$ , given an  $\varepsilon > 0$ , there exist an  $n \in \mathbb{N}$  and a PQC  $W_b(\mathbf{x})$  with width  $O(d \log n)$ , depth  $O(dn^d \log n)$  and the number of trainable parameters  $O(dn^d)$  such that*

$$|f(\mathbf{x}) - f_{W_b}(\mathbf{x})| \leq \varepsilon \quad (\text{C.8})$$

for all  $\mathbf{x} \in [0, 1]^d$ , where  $f_{W_b}(\mathbf{x}) := \langle 0 | W_b^\dagger(\mathbf{x}) Z^{(0)} W_b(\mathbf{x}) | 0 \rangle$ .

*Proof.* Remark S2 has established the uniform convergence of the Bernstein polynomial towards any continuous function within the cubic domain  $[0, 1]^d$ , denoted as  $B_n(f; \mathbf{x})$ , with the property that  $B_n(f; \mathbf{x}) \rightarrow f(\mathbf{x})$  as  $n \rightarrow +\infty$ . Building on Lemma S9, we can effectively implement this Bernstein polynomial  $B_n(f; \mathbf{x})$  using  $f_{W_b}(\mathbf{x})$ . The depth of the PQC  $W_b(\mathbf{x})$  is  $O(dn^d \log n)$ , the width is  $O(d \log n)$ , and the number of parameters is  $O(dn^d)$ . This completes the proof.  $\square$

**Theorem 2.** *Given a Lipschitz continuous function  $f : [0, 1]^d \rightarrow [-1, 1]$  with a Lipschitz constant  $\ell$ , for any  $\varepsilon > 0$  and  $n \in \mathbb{N}$ , there exists a PQC  $W_b(\mathbf{x})$  with such that  $f_{W_b}(\mathbf{x}) := \langle 0 | W_b^\dagger(\mathbf{x}) Z^{(0)} W_b(\mathbf{x}) | 0 \rangle$  satisfies*

$$|f(\mathbf{x}) - f_{W_b}(\mathbf{x})| \leq \varepsilon + 2 \left( \left( 1 + \frac{\ell^2}{n\varepsilon^2} \right)^d - 1 \right) \leq \varepsilon + d2^d \frac{\ell^2}{n\varepsilon^2} \quad (\text{C.9})$$

for all  $\mathbf{x} \in [0, 1]^d$ . The width of the PQC is  $O(d \log n)$ , the depth is  $O(dn^d \log n)$ , and the number of parameters is  $O(dn^d)$ .

*Proof.* Lemma S8 has established the uniform convergence rate of the Bernstein polynomial towards any Lipschitz continuous function within the cubic domain  $[0, 1]^d$ . We know that for any Lipschitz continuous function  $f(\mathbf{x})$  with Lipschitz constant  $\ell$ , there exists a Bernstein polynomial  $B_n(f; \mathbf{x})$  satisfying

$$|f(\mathbf{x}) - B_n(f; \mathbf{x})| \leq \varepsilon + 2\Gamma \sum_{j=1}^d \binom{d}{j} \left( \frac{\ell^2}{4n\varepsilon^2} \right)^j \leq \varepsilon + 2\Gamma \left( \left( 1 + \frac{\ell^2}{4n\varepsilon^2} \right)^d - 1 \right).$$

Building on Lemma S9, we can effectively implement this Bernstein polynomial  $B_n(f; \mathbf{x})$  using  $f_{W_b}(\mathbf{x})$ . The depth of the PQC  $W_b(\mathbf{x})$  is  $O(dn^d \log n)$ , the width is  $O(d \log n)$ , and the number of parameters is  $O(dn^d)$ . This completes the proof.  $\square$

## Appendix D: Approximating smooth functions via nested PQCs

Other than using a Bernstein polynomial to globally approximate a continuous function, we could also utilize local polynomials to achieve a piecewise approximation. To do this, we follow the path of classical deep neural networks [16, 18, 43], using multivariate Taylor series expansion to approximate a multivariate smooth function  $f$  in some small local region. Let  $\beta = s + r > 0$ ,  $r = (0, 1]$  and  $s = \lfloor \beta \rfloor \in \mathbb{N}$ , for a finite constant  $B_0 > 0$ , the  $\beta$ -Hölder class of functions  $\mathcal{H}^\beta([0, 1]^d, B_0)$  is defined as

$$\mathcal{H}^\beta([0, 1]^d, B_0) = \left\{ f : [0, 1]^d \rightarrow \mathbb{R}, \max_{\|\alpha\|_1 \leq s} \|\partial^\alpha f\|_\infty \leq B_0, \max_{\|\alpha\|_1 = s} \sup_{\mathbf{x} \neq \mathbf{y}} \frac{|\partial^\alpha f(\mathbf{x}) - \partial^\alpha f(\mathbf{y})|}{\|\mathbf{x} - \mathbf{y}\|_2^r} \leq B_0 \right\}, \quad (\text{D.1})$$

where  $\partial^\alpha = \partial^{\alpha_1} \dots \partial^{\alpha_d}$  for  $\alpha = (\alpha_1, \dots, \alpha_d) \in \mathbb{N}^d$ . By definition, for a function  $f \in \mathcal{H}^\beta([0, 1]^d, B_0)$ , when  $\beta \in (0, 1)$ ,  $f$  is a Hölder continuous function with order  $\beta$  and Hölder constant  $B_0$ ; when  $\beta = 1$ ,  $f$  is a Lipschitz function with Lipschitz constant  $B_0$ ; when  $\beta > 1$ ,  $f$  belongs to the  $C^s$  class of functions whose  $s$ -th partial derivatives exist and are bounded.

We utilize the following lemma on the Taylor expansion of  $\beta$ -Hölder functions as a mathematical tool for constructing and analyzing the PQC approximation.

**Lemma S10** ([16]). *Given a function  $f \in \mathcal{H}^\beta([0, 1]^d, 1)$  with  $\beta = r + s$ ,  $r \in (0, 1]$  and  $s \in \mathbb{N}^+$ , for any  $\mathbf{x}, \mathbf{x}_0 \in [0, 1]^d$ , we have*

$$\left| f(\mathbf{x}) - \sum_{\|\alpha\|_1 \leq s} \frac{\partial^\alpha f(\mathbf{x}_0)}{\alpha!} (\mathbf{x} - \mathbf{x}_0)^\alpha \right| \leq d^s \|\mathbf{x} - \mathbf{x}_0\|_2^\beta, \quad (\text{D.2})$$

where  $\alpha! = \alpha_1! \dots \alpha_d!$ .

Next, we show how to construct PQCs to implement the Taylor expansion of  $\beta$ -Hölder functions.

### 1. Localization via PQC

As shown in Eq. (D.2), the Taylor expansion of a multivariate smooth function only converges in a fairly small local region, we need to first localize the entire region  $[0, 1]^d$ . Given  $K \in \mathbb{N}$  and  $\Delta \in (0, \frac{1}{3K})$ , for each  $\boldsymbol{\eta} = (\eta_1, \dots, \eta_d) \in \{0, 1, \dots, K-1\}^d$ , we define

$$Q_{\boldsymbol{\eta}} := \left\{ \mathbf{x} = (x_1, \dots, x_d) : x_i \in \left[ \frac{\eta_i}{K}, \frac{\eta_i + 1}{K} - \Delta \cdot 1_{\eta_i < K-1} \right] \right\}. \quad (\text{D.3})$$

By the definition of  $Q_{\boldsymbol{\eta}}$ , the region  $[0, 1]^d$  is approximately divided into small hypercubes  $\bigcup_{\boldsymbol{\eta}} Q_{\boldsymbol{\eta}}$  and some trifling region  $\Lambda(d, K, \Delta) := [0, 1]^d \setminus (\bigcup_{\boldsymbol{\eta}} Q_{\boldsymbol{\eta}})$ , as illustrated in Fig. 2 in the main text. Then we need to construct a PQC that maps any  $x \in Q_{\boldsymbol{\eta}}$  to some fixed point  $x_{\boldsymbol{\eta}} = \frac{\boldsymbol{\eta}}{K} \in Q_{\boldsymbol{\eta}}$ , i.e., approximating the piecewise-constant function  $D(\mathbf{x}) = \frac{\boldsymbol{\eta}}{K}$  if  $\mathbf{x} \in Q_{\boldsymbol{\eta}}$ , where  $\frac{\boldsymbol{\eta}}{K} = (\eta_1/K, \dots, \eta_d/K)$ . We consider the case of  $d = 1$ , where the localization function is

$$D(x) = \frac{k}{K}, \quad \text{if } x \in \left[ \frac{k}{K}, \frac{k+1}{K} - \Delta \cdot 1_{k < K-1} \right] \text{ for } k = 0, 1, \dots, K-1. \quad (\text{D.4})$$

The multivariate case could be easily generalized by applying  $D(x)$  to each variable  $x_j$ . The idea is to find a polynomial that approximates the sign function

$$\text{sgn}(x - c) = \begin{cases} 1, & \text{if } x > c, \\ 0, & \text{if } x = c, \\ -1, & \text{if } x < c \end{cases}, \quad (\text{D.5})$$

as shown in the following lemma.

**Lemma S11** (Polynomial approximation to the sign function  $\text{sgn}(x - c)$  [44]).  $\forall c \in [-1, 1], \Delta > 0, \varepsilon \in (0, 1)$ . *there exists an odd polynomial  $P_{\Delta, \varepsilon}(x)$  of degree  $n = O(\frac{1}{\Delta} \log \frac{1}{\varepsilon})$  that satisfies*

1.  $|P_{\Delta, \varepsilon}(x - c)| \leq 1$  for all  $x \in [-1, 1]$ ,
2.  $|\text{sgn}(x - c) - P_{\Delta, \varepsilon}(x - c)| \leq \varepsilon$  for all  $x \in [-1, 1] \setminus (c - \frac{\Delta}{2}, c + \frac{\Delta}{2})$ .

Note that we could also approximate the step function defined as  $\text{stp}(x - c) := \frac{1}{2} \text{sgn}(x - c) + \frac{1}{2}$  by the polynomial  $P'_{\Delta, \varepsilon}(x - c) = \frac{1}{2} P_{\Delta, \varepsilon}(x - c) + \frac{1}{2}$  of degree  $n = O(\frac{1}{\Delta} \log \frac{1}{\varepsilon})$ , which satisfies that  $|P'_{\Delta, \varepsilon}(x - c)| \leq 1$  for all  $x \in [-1, 1]$  and  $|\text{stp}(x - c) - P'_{\Delta, \varepsilon}(x - c)| \leq \frac{\varepsilon}{2}$  for all  $x \in [-1, 1] \setminus (c - \frac{\Delta}{2}, c + \frac{\Delta}{2})$ . Note that the polynomial  $P'_{\Delta, \varepsilon}(x - c)$  does not have definite parity, and thus cannot be directly implemented by a PQC as shown in Corollary S2. Since only the domain  $[0, 1]$  is relevant to  $x$ , for  $c \in (0, 1)$ , we could define an even polynomial

$$P_{c, \Delta, \varepsilon}^{\text{even}}(x) = \frac{1}{1 + \frac{\varepsilon}{2}} (P'_{\Delta, \varepsilon}(x - c) + P'_{\Delta, \varepsilon}(-x - c)) \quad (\text{D.6})$$

such that  $|P_{c, \Delta, \varepsilon}^{\text{even}}(x)| \leq 1$  for all  $x \in [-1, 1]$  and  $|\text{stp}(x - c) - P_{c, \Delta, \varepsilon}^{\text{even}}(x)| \leq \frac{\varepsilon}{2}$  for all  $x \in [0, 1] \setminus (c - \frac{\Delta}{2}, c + \frac{\Delta}{2})$ . The piecewise-constant function  $D(x)$  can be written as a combination of step functions,

$$D(x) = \sum_{k=1}^{K-1} \frac{1}{K} \text{stp}(x - \frac{k}{K} + \frac{\Delta}{2}). \quad (\text{D.7})$$

Then we could find even polynomials  $P_{c, \Delta, \varepsilon}^{\text{even}}(x)$  that approximate  $\text{stp}(x - \frac{k}{K} + \frac{\Delta}{2})$  for each  $k$ . Combining those polynomials together as in Eq. (D.7), we have the following lemma.

**Lemma S12.** *Given  $K \in \mathbb{N}$  and  $\Delta \in (0, \frac{1}{3K})$ , there exists an even polynomial  $P_{\Delta, \varepsilon}(x)$  of degree  $n = O(\frac{1}{\Delta} \log \frac{K}{\varepsilon})$  that satisfies*

1.  $|P_{\Delta, \varepsilon}(x)| \leq 1$  for all  $x \in [-1, 1]$ ,
2.  $|D(x) - P_{\Delta, \varepsilon}(x)| \leq \varepsilon$  for all  $x \in \bigcup_{k=0}^{K-1} [\frac{k}{K}, \frac{k+1}{K} - \Delta \cdot 1_{k < K-1}]$ .

Note that we could shift the polynomial  $P_{\Delta, \varepsilon}(x)$  such that  $P_{\Delta, \varepsilon}(x) - D(x) \in (0, \varepsilon)$  without changing the degree. It follows that we can construct a PQC to implement the polynomial  $P_{\Delta, \varepsilon}(x)$  by Corollary S2.

**Corollary S13.** *Given  $K \in \mathbb{N}$ ,  $\Delta \in (0, \frac{1}{3K})$  and  $\varepsilon \in (0, \frac{1}{K})$ , there exists a single-qubit PQC  $U_D(x)$  of depth  $O(\frac{1}{\Delta} \log \frac{K}{\varepsilon})$  that satisfies*

$$\langle +|U_D(x)|+ \rangle - \frac{k}{K} \in (0, \varepsilon) \quad \text{if } x \in \left[ \frac{k}{K}, \frac{k+1}{K} - \Delta \cdot 1_{k < K-1} \right] \text{ for } k = 0, 1, \dots, K-1. \quad (\text{D.8})$$

Note that  $\varepsilon$  has to be bounded by  $\frac{1}{K}$ , which is the length of the localized region. We could further implement such a localization procedure for  $\mathbf{x} = (x_1, \dots, x_d)$  on the region  $[0, 1]^d$  by applying the PQC for each  $x_j$ , as stated in the following corollary.

**Lemma S14** (Localization via PQC). *Given  $K \in \mathbb{N}$ ,  $\Delta \in (0, \frac{1}{3K})$  and  $\varepsilon \in (0, \frac{1}{K})$ , there exists a PQC  $W_D(\mathbf{x})$  of width  $O(d)$  and depth  $O(\frac{1}{\Delta} \log \frac{K}{\varepsilon})$  implementing a localization function  $f_{W_D}(\mathbf{x}) : \mathbb{R}^d \rightarrow \mathbb{R}^d$  such that*

$$\mathbf{0} \leq f_{W_D}(\mathbf{x}) - \frac{\boldsymbol{\eta}}{K} \leq \boldsymbol{\varepsilon} \quad \text{if } \mathbf{x} \in Q_{\boldsymbol{\eta}}, \quad (\text{D.9})$$

where  $\mathbf{0} = (0, \dots, 0)$  and  $\boldsymbol{\varepsilon} = (\varepsilon, \dots, \varepsilon)$  are  $d$ -dimensional vectors.

*Proof.* We construct a  $d$ -qubit PQC  $W_D(\mathbf{x}) := \bigotimes_{j=1}^d U_D(x_j)$  where the single-qubit PQC  $U_D(x)$  is constructed in Corollary S13. Then we apply the Hadamard test on each  $U_D(x_j)$  to obtain  $f_{U_D}(x_j) := \langle +|U_D(x_j)|+ \rangle$ . Let  $f_{W_D}(\mathbf{x}) := (f_{U_D}(x_1), \dots, f_{U_D}(x_d))$ , which implements the localization function as required.  $\square$

## 2. Implementing the Taylor coefficients by PQC

Next, we use PQC to implement the Taylor coefficients, which is essentially a point-fitting problem. For each  $\boldsymbol{\eta} = (\eta_1, \dots, \eta_d) \in \{0, 1, \dots, K-1\}^d$  and  $\boldsymbol{\alpha}$ , we denote  $\xi_{\boldsymbol{\eta}, \boldsymbol{\alpha}} := \frac{\partial^\alpha f(\frac{\boldsymbol{\eta}}{K})}{\boldsymbol{\alpha}!} \in [-1, 1]$ . Then we could construct the following PQC,

$$U_{co}^\alpha = \sum_{\boldsymbol{\eta}} |\boldsymbol{\eta}\rangle\langle\boldsymbol{\eta}| \otimes R_X(\theta_{\boldsymbol{\eta}, \boldsymbol{\alpha}}), \quad (\text{D.10})$$

where  $|\boldsymbol{\eta}\rangle = |\eta_1\rangle \otimes \dots \otimes |\eta_d\rangle$  and  $\theta_{\boldsymbol{\eta}, \boldsymbol{\alpha}} = 2 \arccos(\xi_{\boldsymbol{\eta}, \boldsymbol{\alpha}})$ . It gives the following lemma.

**Lemma S15.** *Given a  $\beta$ -Hölder smooth function  $f : [0, 1]^d \rightarrow [-1, 1]$ , for any  $\boldsymbol{\alpha} \in \mathbb{N}^d$  and  $\boldsymbol{\eta} \in \{0, 1, \dots, K-1\}^d$ , there exists a PQC  $U_{co}^\alpha$  such that*

$$\langle \boldsymbol{\eta}, 0 | U_{co}^\alpha | \boldsymbol{\eta}, 0 \rangle = \xi_{\boldsymbol{\eta}, \boldsymbol{\alpha}}. \quad (\text{D.11})$$

The width of the PQC is  $O(d \log K)$  and the depth is  $O(K^d)$ .

We note that the state  $|\boldsymbol{\eta}\rangle$  can be prepared using basis encoding according to the results of localization in Lemma S14.

## 3. Implementing multivariate Taylor series by PQC

To implement the multivariate Taylor expansion of a function, we first build a PQC to represent a single term in the Taylor series, which could be done by combining the monomial implementation in Lemma S5 and the Taylor coefficient implementation in Lemma S15. Thus we have the following corollary.

**Corollary S16.** *For any  $\beta$ -Hölder smooth function  $f$ , given an  $\boldsymbol{\alpha} \in \mathbb{N}^d$  with  $\|\boldsymbol{\alpha}\|_1 \leq s$  for  $s \in \mathbb{N}^+$  and an  $\boldsymbol{\eta} \in \{0, 1, \dots, K-1\}^d$ , there exists a PQC  $U_\eta^\alpha(\mathbf{x})$  such that*

$$\langle \boldsymbol{\eta}, 0 | \langle + |^{\otimes d} U_\eta^\alpha(\mathbf{x}) | \boldsymbol{\eta}, 0 \rangle | + \rangle^{\otimes d} = \frac{\partial^\alpha f(\frac{\boldsymbol{\eta}}{K})}{\boldsymbol{\alpha}!} \left(\mathbf{x} - \frac{\boldsymbol{\eta}}{K}\right)^\alpha. \quad (\text{D.12})$$

The width of the PQC is  $O(d \log K)$ , the depth is  $O(K^d + s)$ , and the number of parameters is at most  $K^d + s + d$ .

*Proof.* Let  $U_\eta^\alpha(\mathbf{x}) := U_{co}^\alpha \otimes U^\alpha(\mathbf{x} - \frac{\boldsymbol{\eta}}{K})$ , where  $U_{co}^\alpha$  is defined in Lemma S15 and  $U^\alpha(\mathbf{x} - \frac{\boldsymbol{\eta}}{K})$  is defined in Lemma S5 with changing input from  $\mathbf{x}$  to  $\mathbf{x} - \frac{\boldsymbol{\eta}}{K}$ . Then the corollary directly follows from Lemma S5 and Lemma S15.  $\square$

The next step is to aggregate single Taylor terms together to implement the truncated Taylor expansion of the target function. The method is in the same spirit as what is utilized in Proposition 1, i.e., using LCU to achieve the following (unnormalized) operator,

$$U_t(\mathbf{x}) := \sum_{\|\boldsymbol{\alpha}\|_1 \leq s} U_\eta^\alpha(\mathbf{x}). \quad (\text{D.13})$$

Then we can implement the Taylor expansion of the function  $f$  at point  $\frac{\boldsymbol{\eta}}{K}$  as

$$\langle \boldsymbol{\eta}, 0 | \langle + |^{\otimes d} U_t(\mathbf{x}) | \boldsymbol{\eta}, 0 \rangle | + \rangle^{\otimes d} = \sum_{\|\boldsymbol{\alpha}\|_1 \leq s} \frac{\partial^\alpha f(\frac{\boldsymbol{\eta}}{K})}{\boldsymbol{\alpha}!} \left(\mathbf{x} - \frac{\boldsymbol{\eta}}{K}\right)^\alpha. \quad (\text{D.14})$$

Hence we have the following lemma.

**Lemma S17.** Given a function  $f \in \mathcal{H}^\beta([0, 1]^d, 1)$  with  $\beta = r + s$ ,  $r \in (0, 1]$  and  $s \in \mathbb{N}^+$ , for any  $\boldsymbol{\eta} \in \{0, \dots, K-1\}^d$ , there exists a PQC  $W_e(\mathbf{x}, \frac{\boldsymbol{\eta}}{K})$  such that  $f_{W_e}(\mathbf{x}) := \langle 0 | W_e^\dagger(\mathbf{x}) Z^{(0)} W_e(\mathbf{x}) | 0 \rangle$  implements the truncated Taylor expansion at point  $\frac{\boldsymbol{\eta}}{K}$ ,

$$f_{W_e}(\mathbf{x}) = \sum_{\|\boldsymbol{\alpha}\|_1 \leq s} \frac{\partial^\alpha f(\frac{\boldsymbol{\eta}}{K})}{\boldsymbol{\alpha}!} (\mathbf{x} - \frac{\boldsymbol{\eta}}{K})^\alpha. \quad (\text{D.15})$$

The depth of the PQC is  $O(s^2 d^s K^d (\log s + s \log d + d \log K))$ , the width is  $O(d \log K + \log s + s \log d)$ , and the number of parameters is  $O(sd^s (s + d + K^d))$ .

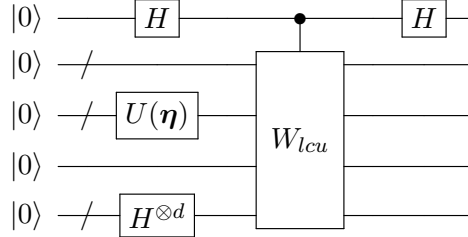
*Proof.* The idea of constructing the PQC  $W_e(\mathbf{x}, \frac{\boldsymbol{\eta}}{K})$  is similar to the construction of  $W_p(\mathbf{x})$  in Proposition 1. The only difference is that here we apply LCU on unitaries  $U_\eta^\alpha(\mathbf{x}) := U_{co}^\alpha \otimes U^\alpha(\mathbf{x} - \frac{\boldsymbol{\eta}}{K})$  instead of  $U^\alpha(\mathbf{x})$ . Thus the controlled unitary is

$$U_c(\mathbf{x}, \frac{\boldsymbol{\eta}}{K}) = \sum_{j=1}^T |j\rangle\langle j| \otimes U_\eta^{\alpha^{(j)}}(\mathbf{x}) \quad (\text{D.16})$$

and the unitary  $W_{lcu}(\mathbf{x}, \frac{\boldsymbol{\eta}}{K}) = (F^\dagger \otimes I) U_c(\mathbf{x}, \frac{\boldsymbol{\eta}}{K}) (F \otimes I)$  satisfies that

$$\langle 0 | \langle \boldsymbol{\eta}, 0 | \langle + |^{\otimes d} W_{lcu}(\mathbf{x}, \frac{\boldsymbol{\eta}}{K}) | 0 \rangle | \boldsymbol{\eta}, 0 \rangle | + \rangle^{\otimes d} = \sum_{\|\boldsymbol{\alpha}\|_1 \leq s} \frac{\partial^\alpha f(\frac{\boldsymbol{\eta}}{K})}{\boldsymbol{\alpha}!} (\mathbf{x} - \frac{\boldsymbol{\eta}}{K})^\alpha. \quad (\text{D.17})$$

We then apply the Hadamard test on  $W_{lcu}(\mathbf{x}, \frac{\boldsymbol{\eta}}{K})$ , giving the quantum circuit  $W_e(\mathbf{x}, \frac{\boldsymbol{\eta}}{K})$  as below



where the unitary  $U(\boldsymbol{\eta})$  takes  $\boldsymbol{\eta}$  as input and maps  $|0\rangle$  to  $|\boldsymbol{\eta}\rangle$ . Note that the controlled unitary  $U_c(\mathbf{x}, \frac{\boldsymbol{\eta}}{K})$  could be implemented by  $O(T(s+1))$  number of  $(\log T)$ -qubit controlled gates and  $O(TK^d)$  number of  $(\log T + d \log K)$ -qubit controlled gates. An  $n$ -qubit controlled gate could be implemented by a quantum circuit consisting of CNOT gates and single-qubit gates with depth  $O(n)$  [38]. Thus  $U_c(\mathbf{x})$  could be implemented by a quantum circuit with depth  $O((s+1)T \log T + TK^d(\log T + d \log K))$  and width  $O(d + \log T + d \log K)$ . Then the depth and width of  $W_{lcu}(\mathbf{x}, \frac{\boldsymbol{\eta}}{K}) = (F^\dagger \otimes I) U_c(\mathbf{x}, \frac{\boldsymbol{\eta}}{K}) (F \otimes I)$  are in the same order of  $U_c(\mathbf{x}, \frac{\boldsymbol{\eta}}{K})$  since  $F$  is simply tensor of Hadamard gates. Therefore the entire depth of the circuit  $W_e$  is  $O((sT \log T + TK^d(\log T + d \log K)))$  and the width is  $O(d + \log T + d \log K)$ . As  $T \leq (s+1)d^s$ , we have the depth and width of PQC shown in Lemma S17. Note that the number of parameters in the PQC equals the number of parameters in  $U_c(\mathbf{x})$ , which is  $O(T(s + d + K^d))$ .  $\square$

Finally, we combine the step of localization and the Taylor series implementation together to achieve a local Taylor expansion for the target function. The PQC is in a nested structure consisting of a PQC for localization PQC and a PQC for Taylor series, see the detailed construction in the following theorem.

**Theorem 3.** Given a function  $f \in \mathcal{H}^\beta([0, 1]^d, 1)$  with  $\beta = r + s$ ,  $r \in (0, 1]$  and  $s \in \mathbb{N}^+$ , for any  $K \in \mathbb{N}$  and  $\Delta \in (0, \frac{1}{3K})$ , there exists a PQC  $W_t(\mathbf{x})$  such that  $f_{W_t}(\mathbf{x}) := \langle 0 | W_t^\dagger(\mathbf{x}) Z^{(0)} W_t(\mathbf{x}) | 0 \rangle$  satisfies

$$|f(\mathbf{x}) - f_{W_t}(\mathbf{x})| \leq d^{s+\beta/2} K^{-\beta} \quad (\text{D.18})$$

for  $\mathbf{x} \in \bigcup_{\eta} Q_{\eta}$ . The width of the PQC is  $O(d \log K + \log s + s \log d)$ , the depth is  $O(s^2 d^s K^d (\log s + s \log d + d \log K)) + \frac{1}{\Delta} \log K$ , and the number of parameters is  $O(sd^s(s + d + K^d))$ .

*Proof.* By Lemma S10, we have the following error bound for  $\mathbf{x} \in Q_{\eta}$ ,

$$\left| f(\mathbf{x}) - \sum_{\|\alpha\|_1 \leq s} \frac{\partial^{\alpha} f(\frac{\eta}{K})}{\alpha!} (\mathbf{x} - \frac{\eta}{K})^{\alpha} \right| \leq d^s \|\mathbf{x} - \frac{\eta}{K}\|_2^{\beta} \leq d^{s+\beta/2} K^{-\beta}. \quad (\text{D.19})$$

Motivated by this, we first construct a localization PQC  $W_D(x)$  as in Lemma S14 such that

$$\mathbf{0} \leq f_{W_D}(\mathbf{x}) - \frac{\eta}{K} \leq \left( \frac{1}{2K}, \dots, \frac{1}{2K} \right) \quad \text{if } \mathbf{x} \in Q_{\eta}. \quad (\text{D.20})$$

The depth of  $W_D(x)$  is  $O(\frac{1}{\Delta} \log K)$ . We then construct a PQC

$$W_t(\mathbf{x}) := W_e(\mathbf{x}, f_{W_D}(\mathbf{x})), \quad (\text{D.21})$$

where  $W_e$  is the PQC proposed in Lemma S17. Note that the state  $|\eta\rangle$  in Lemma S17 could be prepared by rounding  $f_{W_D}(\eta)K$ , i.e.,  $\eta = \lfloor f_{W_D}(\eta)K \rfloor$ . In other words, the PQC  $W_t(\mathbf{x})$  has a nested structure, consisting of a PQC for localization and a PQC for Taylor series implementation. Then we show that  $f_{W_t}(\mathbf{x}) := \langle 0 | W_t^{\dagger}(\mathbf{x}) Z^{(0)} W_t(\mathbf{x}) | 0 \rangle$  can approximate  $\beta$ -Hölder smooth function  $f$  on  $\bigcup_{\eta} Q_{\eta}$ . By the triangle inequality and Eq. (D.19), we have

$$|f(\mathbf{x}) - f_{W_t}(\mathbf{x})| \leq \left| f_{W_t}(\mathbf{x}) - \sum_{\|\alpha\|_1 \leq s} \frac{\partial^{\alpha} f(f_{W_D}(\mathbf{x}))}{\alpha!} (\mathbf{x} - f_{W_D}(\mathbf{x}))^{\alpha} \right| + d^s \|\mathbf{x} - f_{W_D}(\mathbf{x})\|_2^{\beta} \quad (\text{D.22})$$

$$\leq \left| f_{W_t}(\mathbf{x}) - \sum_{\|\alpha\|_1 \leq s} \frac{\partial^{\alpha} f(f_{W_D}(\mathbf{x}))}{\alpha!} (\mathbf{x} - f_{W_D}(\mathbf{x}))^{\alpha} \right| + d^{s+\beta/2} K^{-\beta} \quad (\text{D.23})$$

$$\leq d^{s+\beta/2} K^{-\beta}. \quad (\text{D.24})$$

The second inequality comes from the fact that  $|\mathbf{x} - f_{W_D}(\mathbf{x})| \leq (\frac{1}{K}, \dots, \frac{1}{K})$  for  $\mathbf{x} \in Q_{\eta}$ . This completes the proof.  $\square$

Note that the PQC in Theorem 3 is nesting of two PQCs, while its depth is counted as the sum of two PQCs for simplicity. We have established the uniform convergence property of PQCs for approximating Hölder smooth function on  $[0, 1]^d$  except for the trifling region  $\Lambda(d, K, \Delta)$ . Note that the Lebesgue measure of such a trifling region is no more than  $dK\Delta$ . We can set  $\Delta = K^{-d}$  with no influence on the size of the constructed PQC in Theorem 3. Since  $\nu$  is absolutely continuous with respect to the Lebesgue measure, we have the following corollary.

**Corollary S18.** *Given a function  $f \in \mathcal{H}^{\beta}([0, 1]^d, 1)$  with  $\beta = r + s$ ,  $r \in (0, 1]$  and  $s \in \mathbb{N}^+$ , for any  $K \in \mathbb{N}$  and  $\Delta \in (0, \frac{1}{3K})$ , there exists a PQC  $W_t(\mathbf{x})$  such that  $f_{W_t}(\mathbf{x}) := \langle 0 | W_t^{\dagger}(\mathbf{x}) Z^{(0)} W_t(\mathbf{x}) | 0 \rangle$  satisfies*

$$\|f(\mathbf{x}) - f_{W_t}(\mathbf{x})\|_{L^2(\nu)}^2 = \int_{[0,1]^d} (f(\mathbf{x}) - f_{W_t}(\mathbf{x}))^2 \nu(x) dx \quad (\text{D.25})$$

$$= \int_{\bigcup_{\eta} Q_{\eta} \cup \Lambda(d, K, \Delta)} (f(\mathbf{x}) - f_{W_t}(\mathbf{x}))^2 \nu(x) dx \quad (\text{D.26})$$

$$\leq (d^{s+\beta/2} K^{-\beta})^2 + 4dK^{1-d}. \quad (\text{D.27})$$

The width of the PQC is  $O(d \log K + \log s + s \log d)$ , the depth is  $O(s^2 d^s K^d (\log s + s \log d + d \log K)) + \frac{1}{\Delta} \log K$ , and the number of parameters is  $O(sd^s(s + d + K^d))$ .

TABLE S1. Comparison of approximation errors of PQC and ReLU FNNs for continuous functions

Approach	Target	Width	Depth	Number of parameters	Approximation error
Global PQC	Monomial	$O(d)$	$O(d + s)$	$O(s + d)$	0
ReLU FNN [18]	Monomial	$O(N)^i$	$O(s^2 M)$	$O(s^4 N^2 M)$	$O(sN^{-sM})$
Global PQC	Lipschitz	$O(d \log n)$	$O(dn^d \log n)$	$O(dn^d)$	$2\left(\left(1 + \frac{\ell^2}{n\varepsilon^2}\right)^d - 1\right) + \varepsilon$
Local PQC	Lipschitz	$O(d \log K)$	$O(K^d d \log K)$	$O(K^d)$	$\sqrt{d}K^{-1}$
ReLU FNN [19]	Lipschitz	$O(N)^{ii}$	$O(M)$	$O(K^{d/2} N)^{iii}$	$O(\sqrt{d}K^{-1})$
Local PQC	$\beta$ -Hölder	$O(d \log K + s \log d)$	$O(K^d d^s s^2 \log K)$	$O(sd^s K^d)$	$d^{s+\beta/2} K^{-\beta}$
ReLU FNN [18]	$C^s$ Smooth	$O(s^d dN \log N)$	$O(M \log M)$	$O(s^{2d} d^2 K^{d/2} N)$	$O(s^d K^{-s})$

<sup>i</sup>  $N > d$  by default.

<sup>ii</sup> Assuming that  $8dN^{1/d} + 3d \leq 16N + 30$ .

<sup>iii</sup> Satisfying that  $NM \approx K^{d/2}$ .

#### 4. Comparison of “global” and “local” approaches in this work

We note that we have presented two distinct methodologies for constructing PQC models with UAP properties aimed at approximating continuous functions. In Theorem 2 and Theorem 3, we establish PQC models, guided by the multivariate Bernstein polynomials and the Taylor expansion of multivariate continuous functions, respectively. We categorize these approaches as “local” and “global”. We proceed to conduct a comprehensive comparative analysis of these two strategies in the context of approximating Lipschitz continuous functions, as summarized in Table S1. For the subsequent analysis, we set  $\beta = 1$  thus  $s = 0$  in Theorem 3, in accordance with the Lipschitz continuous property exhibited by the target function.

The approximation error associated with the global approach can be bounded as  $(2^d d \ell^2)/(n\varepsilon^2) + \varepsilon$ . By selecting  $n = (2^d d \ell^2)/\varepsilon^3$ , we ensure an approximation error of  $2\varepsilon$ . Concurrently, the corresponding number of trainable parameters scale as  $O(2^{d^2} d^{d+1} \ell^{2d}/\varepsilon^{3d})$ . In contrast, the local approach exhibits an approximation error scaling as  $\sqrt{d}K^{-1} + \varepsilon$ . Setting  $K = \sqrt{d}/\varepsilon$  ensures an  $2\varepsilon$  approximation error, with the number of trainable parameters scaling as  $O(d^{d/2}/\varepsilon^d)$ . These findings highlight the advantage of the local approach for approximating continuous functions. More importantly, the approximation error proposed by the local method approaches the optimal convergence rate established in Shen *et al.* [19]. A formal comparison between PQCs and classical deep neural networks is stated in the next section.

#### Appendix E: Comparison with related works in classical machine learning

In this subsection, we conduct a comparative exploration of PQCs and classical deep neural networks, focusing on critical aspects including model size, the number of trainable parameters, and approximation error. To establish a meaningful benchmark, we turn our attention to deep feed-forward neural networks (FNNs) distinguished by the incorporation of rectified linear unit (ReLU) activation functions. FNNs represent the foundational class of neural networks, characterized by a unidirectional flow of information, commencing from the input layer and traversing through one or more hidden layers before culminating at the output layer. This architectural design ensures the absence of cyclic dependencies or loops among nodes within each layer. The ReLU activation function, mathematically defined as  $\text{ReLU}(x) := \max(x, 0)$ , has gained prominence across diverse domains, including but not limited to image recognition [61, 62] and natural language processing [63, 64]. Its popularity in feed-forward networks stems from its efficacy in facilitating the convergence of function approximation during network training. Additionally, a recent study [65] has affirmed that classical neural networks employing commonly utilized activation functions can be effectively approximated by ReLU-activated networks, all while maintaining a mild increment in

network size. Readers are also referred to some other excellent works related to ReLU networks [66–68].

In particular, Shen *et al.* [19] have proposed the optimal approximation error to approximate any Lipschitz function. Lu *et al.* [18] have provided a nearly optimal approximation error to approximate any smooth function using ReLU FNNs. For clarity, the comparison of our results with theirs is summarized in Table S1. It is pertinent to observe that, in the majority of practical instances, the smoothness coefficient  $s$  of the target function tends to be modest since most functions to be approximated is not very smooth. Additionally, within practical scenarios, particularly in domains like image recognition and natural language processing, the dimensionality  $d$  of input data is substantially large. Consequently, within this context, we identify terms that solely rely on the variable  $s$  as constants and  $d \gg s$  within Table S1.

We extend our investigation by quantifying the performance of PQC and FNNs in terms of the model size and the number of parameters for approximating continuous functions. Notably, we discover that in cases where the target function adheres to certain norms of smoothness, PQCs exhibit a notable advantage in approximating this function in terms of the model size and the number of parameters.

**Model size.** In particular, we explore the comparison of PQC and FNN model sizes when they yield similar approximation errors. Here, we use a straightforward measure, the product of width and depth, to gauge the model size. By setting approximation error as  $\varepsilon$ , the size of PQC and FNN scale as  $O(d^{3d/2}\varepsilon^{-d/s})$  and  $O(s^{d^2/(2s)}\varepsilon^{-d/(2s)})$ , respectively.

Remarkably, when  $s = \Omega(d^{3s/d}(1/\varepsilon)^{1/d})$ , an intriguing observation emerges: the ratio of model sizes between PQCs and FNNs exhibits a scaling behavior of  $(1/2)^d$ . Our comprehensive analysis leads to the compelling conclusion that in situations where the smoothness threshold is satisfied, PQCs boast a significantly smaller model size compared to FNNs. This highlights a distinctive and pronounced advantage of PQCs over their classical counterparts.

**Number of trainable parameters.** In the present investigation, we delve into the comparative analysis of the number of trainable parameters of PQC and FNN under the premise of yielding comparable approximation errors. From the perspective of approximation theory, the count of parameters serves as a standard metric for assessing model degrees of freedom and expressing model expressiveness. By setting approximation error as  $\varepsilon$ , the number of trainable parameters of PQC and FNN scale as  $O(d^{3d/2}\varepsilon^{-d/s})$  and  $O(s^{d^2/(2s)}\varepsilon^{-d/(2s)}N)$ , respectively. Here, the hyperparameter  $N$  signifies FNN’s width, while  $M$  signifies its depth, and both satisfy  $NM \approx K^{d/2}$ . With  $N \approx K^{\lambda_0 d/2}$  and  $M \approx K^{\lambda_1 d/2}$  complying with  $\lambda_0 + \lambda_1 = 1$  and  $\lambda_i \in (0, 1)$  for  $\forall i \in \{0, 1\}$ .

Remarkably, through our analysis, we have uncovered that when  $s = \Omega((d^{3s/d}(1/\varepsilon)^{(1-\lambda_0)/d})^{1/(1+\lambda_0)})$ , the relationship between the number of trainable parameters of PQCs and FNNs demonstrates a scaling pattern characterized by  $(1/2)^d$ . As a consequence, the number of trainable parameters of PQCs significantly reduces compared to that of FNNs. This revelation solidifies the prospect of a quantum advantage over FNNs, particularly for target functions that adhere to specific smoothness criteria. Moreover, it is of paramount significance to note that as the width of the FNN increases, such criteria related to smoothness can be relaxed, leading to an even more pronounced quantum advantage.

**Approximating monomial.** Here we conduct a comparative performance analysis of PQC and FNN in approximating monomial functions of degree  $s$ . Within this specialized target function space, PQCs exhibit distinct advantages in terms of width, depth, model size, and the number of trainable parameters. Notably, PQCs possess the unique capability to precisely capture the dynamics of monomial functions, eliminating the need for approximation, and thereby offering a compelling advantage. These advantages position PQCs as promising candidates for outperforming FNNs when addressing more complex target function spaces.

**Approximating Lipschitz functions.** Here we explore the performance of the PQC and the optimal FNN for approximating Lipschitz functions. While the approximation error derived from our approach converges toward the optimal rate established in Shen *et al.* [19], our analysis reveals that the model size and the number of trainable parameters of the constructed PQC do not manifest any quantum advantage when compared with the optimal ReLU FNN proposed in Shen *et al.* [19]. Specifically, the model size and the

number of trainable parameters of our PQCs align with that of the optimal ReLU FNN when the latter is designed with a constant depth and arbitrary width.